Estuaries and Coasts (2020) 43:909–926
https://doi.org/10.1007/s12237-020-00704-5

Physical and Biogeochemical Factors Driving Spatially Heterogeneous Phytoplankton Blooms in Nearshore Waters of Santa Monica Bay, USA

Beth A. Stauffer[1] · Gaurav S. Sukhatme[2] · David A. Caron[3]

Received: 25 July 2019 / Revised: 9 January 2020 / Accepted: 14 January 2020 / Published online: 5 February 2020

Abstract

Phytoplankton blooms in nearshore waters are difficult to predict using only biogeochemical factors known to control phytoplankton growth, yet the need to understand these events continues to grow with expanding harmful algal bloom (HAB) events. The present study investigated the spatial and temporal dynamics of phytoplankton blooms and their drivers in King Harbor, a harbor in Santa Monica Bay in the Southern California Bight. High-frequency sensor measurements of environmental variables and biomass and discrete sampling of phytoplankton community composition and nutrients over an annual cycle were obtained. Eleven distinct bloom events, nine of which were numerically dominated by dinoflagellates, were identified over the study period. Results from both regression-based and time series analyses show that these blooms were correlated with increased temperature, changes in nutrient concentrations, and decreased tidally driven mixing, revealing an opportunity for bloom initiation close to neap tides. Predictors of chlorophyll biomass and environmental factors that explained differences in microplankton community structure differed between the two basins of King Harbor, despite their close and connected nature. Biomass and HAB taxa abundances in the harbor were significantly correlated with those in Santa Monica Bay with a 1-week lag in the harbor data, suggesting possible onshore transport of organisms into the harbor. The results of this study quantify the significant influence of tidal cycle as a physical process operating locally and at timescales of hours to days and provide evidence for a high degree of spatial heterogeneity in bloom dynamics in nearshore environments.

Keywords Algal blooms · Nearshore environments · Physical forcing · Tidal stirring · Dinoflagellate

Introduction

Harmful algal blooms (HABs) affect coastal and inland waters throughout the USA and globally and are predicted to continue to increase in frequency and severity with ongoing climate change (Doney et al. 2012; Hallegraeff 2010). This increase is due, at least in part, to changes related to eutrophication (Anderson et al. 2002; Kudela et al. 2010; Rabalais et al. 2009) and warming (O'Neil et al. 2012; Paerl et al. 2016; Ryan et al. 2017), among other factors. HABs can have a number of negative effects through a variety of mechanisms (including toxin production) on competing members of plankton communities (e.g., Clough and Strom 2005; Imai 2012; Weissbach et al. 2011; Xu et al. 2015), aquatic food web structure (e.g., Abi-Khalil et al. 2016; Clough and Strom 2005; Colin and Dam 2003; Graham and Strom 2010; Place et al. 2012; Stauffer et al. 2017; Turner and Tester 1997), and animal and human health (e.g., Akmajian et al. 2017; Anderson et al. 2000; Lefebvre et al. 2016; Lewitus et al. 2012; Miller et al. 2010; Trainer et al. 2010).

Improving our understanding of the factors controlling algal blooms, and HABs in particular, requires an ability to both define and detect bloom events and to quantify the important physical and biogeochemical factors creating the conditions for enhanced growth and/or accumulation of algae. The very

Communicated by James L. Pinckney

Electronic supplementary material The online version of this article (https://doi.org/10.1007/s12237-020-00704-5) contains supplementary material, which is available to authorized users.

✉ Beth A. Stauffer
beth.stauffer@louisiana.edu

[1] Department of Biology, University of Louisiana at Lafayette, Lafayette, LA 70503, USA

[2] Viterbi School of Engineering, University of Southern California, Los Angeles, CA 90089, USA

[3] Department of Biological Sciences, University of Southern California, Los Angeles, CA 90089, USA

definition of a bloom, however, is a topic of considerable ongoing debate (Smayda 1997). Definitions and suggested thresholds for bloom designation vary in published studies (Carstensen et al. 2007; Kim et al. 2009; Nezlin et al. 2012; Ryan et al. 2008), many of which are focused on resolving large, seasonally recurring "spring bloom" phenomena (e.g., Brody et al. 2013; Cole et al. 2015; Siegel et al. 2002). In the upwelling-influenced waters of the California Current Ecosystem, Kim et al. (2009) employed both constant and varying threshold designations for blooms using a pier-based chlorophyll-a (Chl) dataset, while Ryan et al. (2008) and Nezlin et al. (2012) considered blooms as occurring when Chl exceeded threshold concentrations based on satellite-derived estimates of biomass (75 mg L^{-1} and 5 mg L^{-1}, respectively). Satellite-based estimates of biomass and bloom designations have also been developed using less derived products, for example, Hu et al. (2005) found strong correlations between patches with fluorescence line height (FLH) values > 0.12 W μm^{-1} sr^{-1} and bloom-level abundances of *Karenia brevis* (> 10^4 cells L^{-1}) off the Florida coast.

While the role of nutrients in stimulating phytoplankton growth, including that of HAB taxa, is relatively well understood (e.g., Glibert et al. 2010; Heisler et al. 2008; Kudela et al. 2010), the roles of physical processes that affect water movement (i.e., mixing, turbulence) have been less resolved. This is especially true in estuaries and nearshore embayments, where physical processes with a wide range of dominant temporal cycles—including storm events (seasonal and episodic), tidal cycles (semidiurnal to fortnightly), and variability in freshwater discharge (seasonal to interannual)—may all be at play. It is also important to note that using satellite estimates of Chl in these nearshore waters is complicated by the effects of land and shallow water columns which interfere with reflectance values (summarized in Nezlin et al. 2012).

The California Current Ecosystem is an upwelling regime with the potential for high levels of primary productivity (Hickey 1979). Within-season variability dominates changes in Chl in the system, especially in inshore areas. Inshore waters are also regions of enhanced primary producer biomass, observed in the Southern California Bight (SCB) as onshore-offshore gradients of Chl in Santa Monica Bay (Corcoran and Shipe 2011) and high incidence of bloom-level Chl in nearshore bands (< 5 km from the coast) throughout the SCB (Nezlin et al. 2012). These inshore waters can also act as areas for enhanced HAB occurrence, documented in Monterey Bay as a nearshore "incubator" for dinoflagellate blooms (Ryan et al. 2009; Ryan et al. 2008) and in San Pedro Bay as "hotspots" for blooms of the diatom *Pseudo-nitzschia* spp. and their associated toxin, domoic acid (Schnetzer et al. 2007; Smith et al. 2018). Coastal phytoplankton and HAB dynamics are also spatially linked, with indications of connectivity among HAB taxa abundances in the bays of the SCB (Bialonski et al. 2016). Additionally, some bloom events in the nearshore waters of SCB have been attributed to short-term (i.e., < 1 week) changes in nutrient availability and/or physical processes (Bialonski et al. 2016; Omand et al. 2012; Omand et al. 2011; Seubert et al. 2013).

To address our gap in understanding HABs in nearshore environments, Ganju et al. (2016) argued that coupled hydrodynamic-ecological models are necessary. Previous studies have shown important relationships between increased water residence time and blooms, for example of toxic dinoflagellates in a Cape Cod, MA estuary (Ralston et al. 2015), in a Brazilian reservoir (Soares et al. 2012), and off the coast of southern California (Nezlin et al. 2012). Other studies have pointed to the potential for increased phytoplankton biomass and blooms during periods of reduced tidally induced mixing (Cloern 1991; Leles et al. 2014; Lucas et al. 1999). Complex or rapidly changing hydrography complicates the detection and documentation of blooms in nearshore and estuarine systems. Blooms in these systems may go undetected with lower frequency sampling efforts (i.e., biweekly-monthly; Egerton et al. 2014), thus necessitating the use of higher frequency and/or continuous sampling approaches (Babin et al. 2005; Cullen 2008; Doucette and Kudela 2017; Ho and Michalak 2015; Kaitala 2019; Stauffer et al. 2019; Zeng and Li 2015).

This study focused on quantifying the contributions of physical processes that drive mixing in nearshore environments—primarily tidal cycling and winds—in combination with temperature, salinity, and dissolved nutrients to the spatial and temporal dynamics of phytoplankton biomass and community composition in a semi-enclosed basin of Santa Monica Bay. The purpose was to understand the extent to which these local, high-frequency physical processes, rather than environmental and physical drivers of phytoplankton blooms operating seasonally and/or over multiple years, contribute to phytoplankton blooms in the nearshore environment. To do this, we employed both high-frequency sensor measurements of environmental variables and biomass and lower frequency sampling of phytoplankton community composition and nutrients through an annual cycle. We also compared results from this study with biomass and abundances of HAB taxa at a nearby, more open-ocean location in Santa Monica Bay to better understand how phytoplankton bloom dynamics near shore are related to larger regional phytoplankton dynamics in this region of the SCB.

Methods

Site Description

King Harbor is a semi-enclosed, recreational harbor within Santa Monica Bay in Los Angeles County, USA (33.847° N 118.397° W; Fig. 1). The harbor consists of northern (NB) and

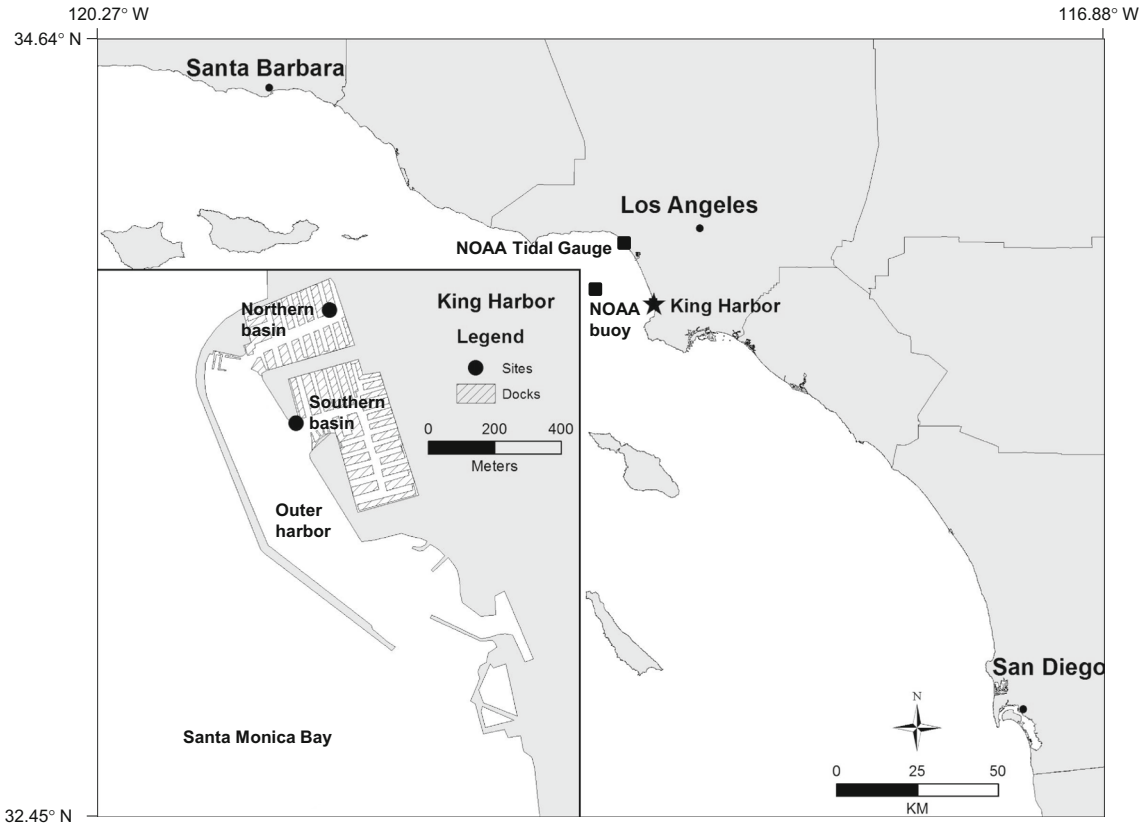

Fig. 1 Map of the Southern California Bight, with star marking location of King Harbor. Black squares indicate locations of the NOAA tide gauge and NDBC buoy from which tide and wind speed, respectively, were obtained. Black dots in the inset of King Harbor indicate sampling locations; the outer harbor region and Santa Monica Bay are also noted

southern basins (SB) adjoined by an outer harbor region that is protected from Santa Monica Bay by a rubble breakwater (Fig. 1). Exchange of water between the outer harbor and adjacent bay is provided primarily via the south-facing harbor channel. Water depths within the harbor range from 3.5 to 6.0 m in the marina basins to 7.0 to 10 m in the outer harbor connecting the basins. There are no natural freshwater inputs into NB; there are, however, 5 storm drains with diameters of 15–94 cm that discharge into SB (documents provided courtesy of the City of Redondo Beach). Terrestrial runoff from these point sources occurs almost exclusively in the rainy season, typically from November to March.

Oceanographic Data

Multi-parameter Water Quality Monitors (WQMS; WETLabs) were deployed from floating docks in NB and SB from May 2010 to June 2011 (Fig. 1). Sensors were deployed at 0.5–1.0 m depth from the surface and programmed to record temperature (°C), salinity (practical salinity units [PSU]), dissolved oxygen (mL L^{-1}), chlorophyll *a* fluorescence (Chl) at 695 nm (μg L^{-1}), and turbidity at 700 nm (NTU) for 10 s at 30-min intervals. The effects of biofouling were minimized by equipping each WQM with a copper BioWiper (WETLabs) installed over the optical sensors and a bleach injection system (BLIS) module, which injected 28 μL 10% bleach into the dissolved oxygen sensor module on an hourly basis (Orrico et al. 2007). In addition to these bio-fouling reduction methods, sensors were cleaned every 2–4 weeks depending on season.

WQM sensors were factory-calibrated prior to deployment. Following deployment, the WQM sensors were cross-calibrated using a 500-gal tank across a range of salinities (5.86–9.47), dissolved oxygen (2.28–4.05 mL L^{-1}), and temperature (23.9 to 24.3 °C). Pairwise least-square linear regressions were calculated for each sensor relative to a sensor designated as the "standard," which was primarily deployed in NB during the 12-month study period. The sensors showed a high level of agreement ($R^2 \geq 0.999$), and the linear regression was used to compute the mathematical relationship between each sensor. The cross-calibration tank procedure did not sufficiently describe differences in the Chl fluorescence sensors, however, primarily due to a lack of range simulated in the tank deployment. The three WQM Chl sensors were therefore compared to each other through calibration to in vitro Chl fluorescence collected from whole (unfiltered) seawater samples at each location on a weekly basis (see "Discrete Water Samples" below). After removing samples collected during

high biomass events, in vitro Chl fluorescence was related by linear regression to an hourly average of WQM Chl fluorescence calculated for each sample. Finally, as a result of necessary repair and sensor replacement during the study period (Oct–Nov 2010), separate regression analyses of Chl fluorescence were performed for each sensor for pre- and post-factory maintenance. Temperature, salinity, dissolved oxygen, and Chl data standardized in this manner were used throughout all subsequent analyses.

Hourly tidal height measurements (relative to mean low water) were obtained from the NOAA Tides and Currents website (http://tidesandcurrents.noaa.gov) for Station 9,410,840 at the Santa Monica Pier (SM Pier) in Santa Monica Bay (34.008° N 118.500° W), approximately 20 km north-northwest of King Harbor (Fig. 1). Tidal height data obtained from the NOAA tidal station were compared to water column height data collected by an upward-looking acoustic Doppler current profiler (ADCP; Sontek Argonaut XR) deployed in the northern basin from in June–July 2008. When datasets were normalized by mean and standard deviation to account for datum differences, a comparison showed excellent agreement in the timing of the tidal cycle in the harbor relative to Santa Monica Bay, with mean residual difference of 9.80×10^{-3} mm (Fig. A1). Hourly meteorological data including wind speed and direction were also retrieved from the NOAA National Data Buoy Center (http://www.ndbc.noaa.gov) for Station 46,221 in Santa Monica Bay (33.854° N 118.633° W) for the period from May 2010 to June 2011 (Fig. 1). Daily upwelling indices for 33° N 199° W were obtained from the NOAA Pacific Fisheries Environmental Lab (www.pfel.noaa.gov/products/PFEL/modeled/indices/upwelling/upwelling) and binned into 7-day averages.

Data Processing

All standardized WQM data were screened for outliers. Outliers can be statistically defined as falling > 2 standard deviations from the mean of the normally distributed dataset (e.g., Wilcox 2003); however, since natural systems may experience valid changes as a result of rapid shifts in environmental conditions, outliers in the WQM dataset were defined as > 5 standard deviations from the dataset mean for each measured parameter. Following outlier removal, data sampled every 30 min over 10 s were binned to hourly means and missing hourly data points were interpolated using the piecewise cubic Hermite polynomial to more properly estimate data that are not necessarily smooth (Fritsch and Carlson 1980). Only short gaps in data (< 2 h) were interpolated to prevent seeding the dataset with false periodicities. As a result, data gaps exist in SB (Oct 29–Dec 1, 2010) and NB (Oct 8–Oct 29, 2010) when sensors were removed for factory repair.

Chl data were further corrected for the effects of non-photochemical quenching (NPQ) using the methods described by Omand et al. (2011) and similar to those used by Todd et al. (2009). A HOBO light sensor (Onset Computer Corporation) was continuously deployed at the surface (unsubmerged) of the northern basin and logged illuminance (units of lux) at 30-min intervals. An empirical linear relationship ($R^2 > 0.999$) was established between the HOBO light sensor and a quantum scalar radiometer (QSL-100 and QSP-170B; Biosciences) at ambient light levels ranging from 78 to 2871 μmol photons m^{-2} s^{-1}. This relationship was used to convert the continuous HOBO light data from the field to surface irradiance (I_0) for use in the NPQ Chl correction, as described below. Two periods of data were missing: May 7–28, 2010 and April 8–May 16, 2011. For these periods, daily irradiance curves were estimated from the respective mean cycles during June 2010 and early April and late May 2011. A median exponential attenuation coefficient (k) of 0.34 m^{-1} was calculated based on daily midday vertical profiles of irradiance taken over the course of 2 weeks in 2008 using the same radiometer (data not shown). Irradiance at sensor depth z (I_z) was estimated using the attenuation coefficient according to Beers Law, and normalized irradiance at depth (relative to the maximum irradiance) was further required to determine the quenching function (Q_z):

$$Q_z = \frac{f}{f + I_z^*} \tag{1.1}$$

Finally, corrected Chl (Chl_z) was calculated from the measured standardized Chl fluorescence (Chl_{mz}) from each WQM sensor using the equation:

$$\mathrm{Chl}_z = \frac{\mathrm{Chl}_{mz}}{Q_z} \tag{1.2}$$

An f value of 1.8 was selected to minimize the correlation of Q_z and Chl_{mz}, a value that is comparable to that (1.6) utilized in Omand et al. (2011) and which yielded Q_z values ranging from 0.64 to 1. Using the above equations, Chl_z was enhanced by up to 56% relative to Chl_{mz} during mid-day/afternoon hours. This range of enhancement is comparable to those (56–100%) reported in Omand et al. (2011) and references therein. Standardized and NPQ-corrected Chl data were used in all subsequent analyses.

Discrete Water Samples

Surface water samples were collected weekly at the two basin sites from May 7, 2010 to June 6, 2011 for dissolved inorganic nutrient concentrations, extracted Chl, and microplankton community composition (Fig. 1). Samples were typically collected before noon, with > 90% collected between 09:00 and 11:00. Acid-washed polycarbonate bottles were rinsed with sample water and filled with surface water taken from < 0.5 m depth and kept cool, vented, and out of direct sunlight until subsampling, typically within 3–4 h. Samples for

dissolved inorganic nutrient analyses were filtered on-site through 0.2-μm syringe filters, with filtrate collected in acid-washed HDPE bottles, and frozen at − 20 °C until analysis. Concentrations of nitrate (incl. of nitrite, detection range 0.2–300 μM), phosphate (0.1–200 μM), and silicate (1.0–600 μM) were measured with ± 5% precision on a QuikChem 8000 flow injection analyzer (Lachat Instruments) by the University of California Santa Barbara Analytical Lab. Subsamples were also filtered in duplicate onto 25-mm glass fiber filters (GFF; Whatman) for in vitro Chl analysis, extracted in 100% acetone at − 20 °C in the dark for 24 h, and run on a calibrated laboratory fluorometer (TD-700, Turner Designs) prior to and following acidification with 5% HCl to correct for phaeopigments (Strickland and Parsons 1972).

Subsamples for analyzing microplankton community composition were preserved with 1% formalin and stored at room temperature in glass bottles in the dark until examination by microscopy after settling in Utermöhl chambers (Utermohl 1931, 1958). Volumes ranging from 5 to 50 mL from each sample were settled for 24–48 h to allow for effective viewing and enumeration. Autotrophs and heterotrophs in the microplankton size class (approx. 20–200 μm) were identified at the genus and class levels, respectively. Samples were counted on an inverted compound microscope (Leica DMIRBE) at × 400 total magnification with a minimum of 200 cells and/or 20 fields of view enumerated for each sample. Microscopical characterization of the microplankton community allowed identification and enumeration of organisms with relatively distinct morphological characteristics that were present at moderate to high abundances. Epifluoresence microscopy using blue light excitation was utilized to differentiate between auto- and heterotrophs where possible. Unidentifiable groups of organisms (e.g., some pennate diatoms, small gymnodinoid dinoflagellates) were classified by size and shape. To better estimate counting error, ten samples were counted in triplicate. Coefficients of variation (CV) ranged from 16% for taxa present at > 50 cells mL^{-1} to 28% for taxa present at > 25 cells mL^{-1} and 38% for taxa present at > 5 cells mL^{-1}. These CVs suggest that all but the rarest taxa (< 5 cells mL^{-1}) were counted accurately. A simple ratio of dinoflagellate vs. diatom dominance (dino:diatom) was calculated based on total cell abundances in each of these classes. Heterotrophic dinoflagellates (e.g., *Noctiluca scintillans*, *Polykrikos* spp.) were not included in the calculation of this ratio.

Comparison to Regional Bloom Dynamics

A dataset of HAB taxa and Chl concentrations at the SM Pier in Santa Monica Bay provided by the Southern California Coastal Ocean Observing System (SCCOOS; http://www.sccoos.org/data/habs/) was used to compare biomass and community composition from the two King Harbor basins with the larger region. SM Pier data that were sampled < 3 days prior to the harbor sampling dates used ($n = 53$). Five HAB taxa were counted in the SCCOOS and harbor datasets: *Akashiwo sanguinea*, *Alexandrium* spp. (primarily *Alexandrium catenella*), *Dinophysis* spp., *Lingulodinium polyedrum*, *Prorocentrum* spp., and *Pseudo-nitzschia* spp. The SCCOOS data identifies the *Pseudo-nitzschia delicatissima* and *Pseudo-nitzschia seriata* groups, based on their distinct profiles as toxin producers (Fernandes et al. 2014). For the purposes of comparison with this study, counts of those two groups were summed.

Statistical Analyses

Contributions of high-frequency, local environmental and physical processes (i.e., tidal cycling, wind, and upwelling) to changes in Chl were investigated using general linear models and time series analyses. Models of Chl in each basin were generated using temperature, phosphate, silicate, nitrate, tidal amplitude, and wind speed as predictor variables. Chl and phosphate were log-transformed. Upwelling index and salinity were not included in the models given their high level of collinearity with nutrient concentrations and general lack of variability, respectively. Dissolved oxygen was not included given its frequent covariance with phytoplankton biomass and the extremely low DO concentrations associated with the spring 2011 fish kill event (Stauffer et al. 2011).

General linear models were fit to each dataset ('fitlm', MATLAB R2018b) using environmental variables measured instantaneously with Chl (i.e., within 1 h of sampling, 0-day lag) and environmental variables averaged over the preceding week (i.e., 7-day lag). A 7-day lag was used due to the limited sampling resolution of nutrient concentrations in the current study, which made it difficult to consider other lags without substantial and possibly unsupported interpolation of those data. Models were run without and with the physical variables (tidal amplitude and wind speed), and overall fit of the models was compared using adjusted R^2 and root mean square error (RMSE). Standard regression diagnostics indicated that there were some minor violations of the assumptions of regression (normality and homoscedasticity of variance). These violations were largely attributable to three data points for each dataset, which were removed, and the regressions were re-run. The regression results without these data points were similar in significance and parameter value to those produced when these data points were included, and the interpretation remained unchanged. We have included the model results that include the three data points in Table A1 (Supplementary Information).

Bivariate relationships between upwelling index and biogeochemical variables were measured using Spearman's rank-order correlations (ρ) to allow for non-linear relationships. Comparison of Chl concentrations and HAB taxa abundances (cells mL^{-1}) at the SCCOOS SM Pier and King Harbor sites

was done by Pearson Product Moment Correlation. Multivariate statistical approaches (PRIMER-e, version 7; Clarke and Gorley 2015) were used to investigate changes in microplankton community composition in the two harbor basins and in HAB taxa abundances between the harbor basins and SM Pier during the study period. Cell abundances were square-root transformed, and assemblages were compared using the Bray-Curtis dissimilarity index (Bray and Curtis 1957), which is not affected by absences of species between samples (Clarke et al. 2014). Resemblance matrices based on the Bray-Curtis coefficient were further used in cluster analysis with similarity profile permutation tests (SIMPROF) to examine if dissimilarities among the assemblages were significant (Clarke et al. 2014) and in non-metric multi-dimensional scaling (nMDS) to graphically represent distinct assemblages in two-dimensional space. The BEST Bio-Env routine was further used to determine which environmental variables best explained among-sample differences in assemblages in each basin (Clarke et al. 2014). A permutation-based test statistic was used to provide a measure of significance of the global bio-Env model ($p < 0.05$; Clarke et al. 2014).

A continuous wavelet transform time series analysis was also used to detect periodic signals in single datasets and provide correlative comparisons of dominant oscillations between two datasets. The wavelet method does assume neither independence of data nor stationarity of the periodicities or correlations over time (Maraun and Kurths 2004; Maraun et al. 2007). Wavelet transforms and coherence analyses were applied to standardized environmental and physical variables and Chl concentrations normalized to the mean and standard deviation of those datasets. Time series analyses were run using the SOWAS package (Maraun et al. 2007; Maraun and Kurths 2004) in MATLAB (Mathworks) using the Morlet continuous wavelet function, which offers a good balance of resolution in both time and frequency (Grinsted et al. 2004). While the Torrence and Compo (1998) method has been utilized in other recent papers (e.g., Blauw et al. 2012; Carey et al. 2016), point-wise significance testing used in that method can lead to high rates of false positives (Maraun et al. 2007). The SOWAS package utilizes more conservative area-wise significance testing that rejects 90% of falsely significant patches that are due to intrinsic correlations in datasets as a result of the reproducing kernel (Maraun et al. 2007). An initial scale of 0.1 day (2.4 h) was used for both continuous wavelet transforms and coherence spectra and scaled up 6 octaves consisting of 12 suboctaves each. For coherence analyses, the time series were smoothed 1 octave in scale and 3 periods in time. Data outside of the cone of influence, an indication of regions of the spectrum sensitive to edge effects, were not used in interpretation. Due to data gaps in fall 2010, wavelet analyses were applied for two periods (May–Oct/Nov 2010 and Oct/Dec 2010–June 2011) that were 5 and 8 months long.

Results

General Oceanographic Conditions in King Harbor

During the 1-year study period, both basins showed seasonally increasing temperatures to maxima above 22 °C in summer (Fig. 2b; Table 1); reductions in salinity associated with storm events from fall to spring (Fig. 2c); peaks in Chl in summer, late winter, and spring (Fig. 2e); and generally higher concentrations of NO_3 and PO_4 in spring months (Fig. 2f, g). Dissolved oxygen was generally high (> 5 mL L^{-1}) throughout the study period (Fig. 2d), with the exception of a pronounced hypoxia event over 3 months in 2011 associated with a fish kill event (Fig. 2d, black box; Stauffer et al. 2012, 2013). The upwelling index was positive for most of the study period, indicating a net volume of water upwelled near the coast that reached maxima of 217 and 282 m^3 s^{-1} 100 m^{-1} in late May 2010 and early June 2011, respectively (Fig. 2h, gray bars). However, monthly upwelling anomalies based on climatological trends were largely negative (Fig. 2h, black circles), suggesting minimal overall upwelling during the study period when compared to interannual and decadal trends. Notable exceptions were in July and November–December 2010 and April 2011, during which upwelling strength was higher than average (Fig. 2h, black circles). Wind speeds were generally moderate (< 5 m s^{-1}), but high wind speeds up to 18.4 m s^{-1} occurred in winter and spring months (Fig. 2i).

Physical oceanographic conditions were generally highly correlated between the two basins throughout the study period (temperature $\rho = 0.986$, salinity $\rho = 0.865$, both $p < 0.01$). Correlation strength between the two basins was lower, however, when Chl ($\rho = 0.538$, $p < 0.01$) or inorganic nutrient concentrations ($\rho = -0.114$–0.671) were considered (Table 2). These differences suggest that NB was, on average, warmer (+ 0.2 °C), with lower minimum salinity (− 1.5), and had higher average nutrient and chlorophyll concentrations (+ 0.31 μg L^{-1} Chl; + 0.97 μM NO_3; + 1.62 μM PO_4, + 9.03 μM SiO_4) than SB (Table 1).

Harbor Bloom Events

Application of the constant threshold approach for designating blooms (> 2 standard deviations from the annual mean; Kim et al. 2009; Seubert et al. 2013) resulted in threshold chlorophyll concentrations of 8.20 μg L^{-1} and 11.59 μg L^{-1}, in SB and NB, respectively. These thresholds indicated the initiation of 11 total blooms (9 and 7 blooms in SB and NB, respectively, Fig. 2e, initiation dates indicated as vertical gray lines), while the varying threshold approach (Kim et al. 2009) increased those numbers dramatically (up to 300 bloom initiation dates). Blooms were identified in the months of May, June, and December 2010 and January, March, April,

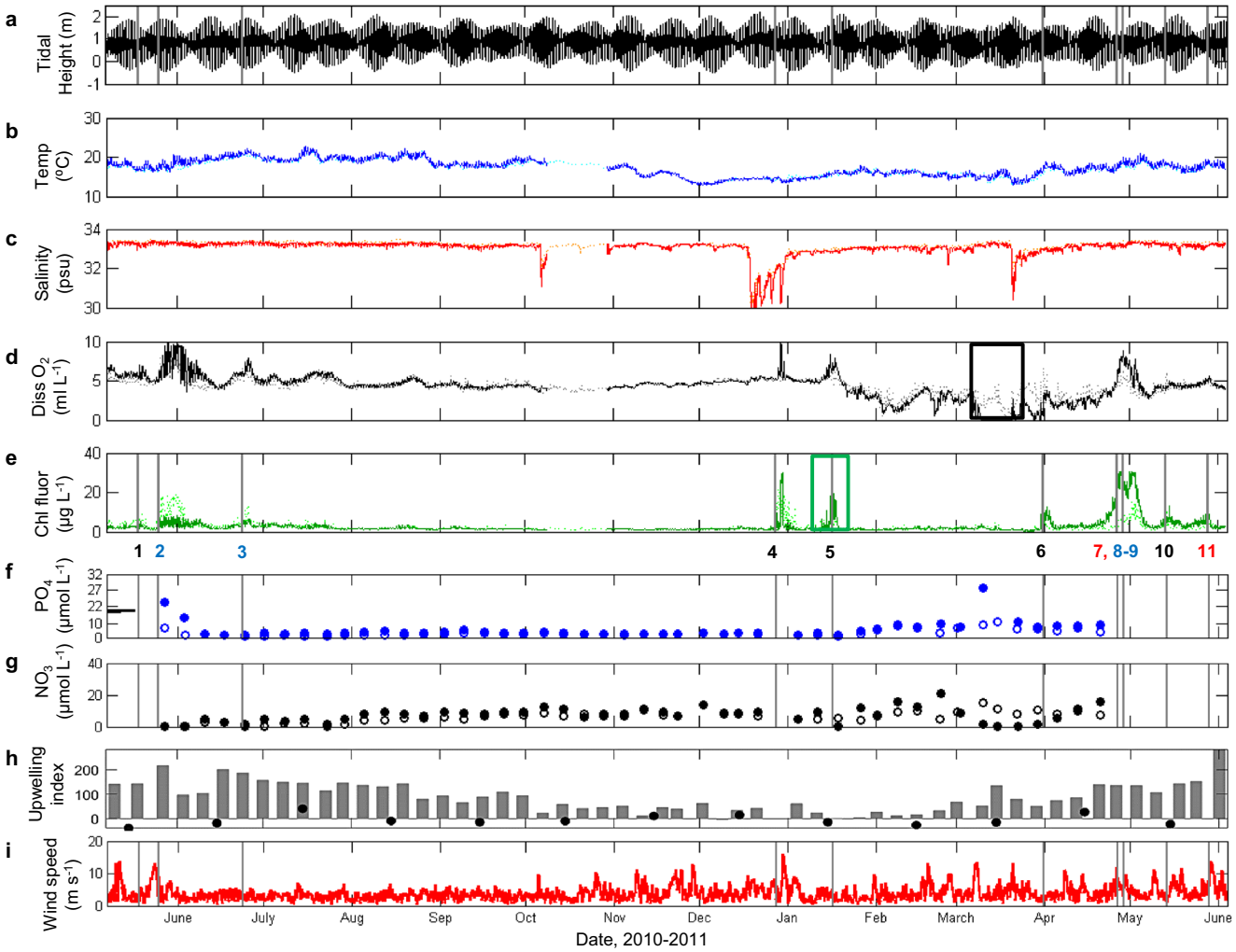

Fig. 2 Time series of tidal height (**a**), temperature (**b**), salinity (**c**), dissolved oxygen (**d**), corrected chlorophyll fluorescence (**e**), dissolved PO_4 (**f**), dissolved $NO_3 + NO_2$ (**g**), upwelling index (**h**), and 6-h averaged wind speed (**i**) in the NB (solid lines) and SB (lighter, dashed lines) of King Harbor from May 2010 to 2011. Units for parameters are as follows: tidal height (m from mean low water), temperature (°C), salinity (psu), dissolved oxygen (mL L^{-1}), chlorophyll fluorescence (µg L^{-1}), dissolved PO_4 and $NO_3 + NO_2$ (µM), upwelling index (m^3 s^{-1} of water transporter 100 m^{-1} of coastline), and wind speed (m s^{-1}). Upwelling index binned to a 7-day average (gray bars) and upwelling anomaly calculated relative to monthly climatological means (black dots) are presented (**h**). Vertical gray lines in tidal amplitude, chlorophyll, nutrient, and wind speed plots indicate date of initiation of bloom events. Blue numbers indicate bloom events occurring in only SB, red numbers indicate bloom events occurring in only NB, and black numbers indicate bloom events occurring in both basins. The black and green boxes in **d** and **e** represent the hypoxia-fish kill event and *Eutreptiella* bloom, respectively (see "Results")

and May 2011 (Fig. 2). Five of the blooms occurred simultaneously in both basins of the harbor (Fig. 2e, black numerals), while four occurred only in SB (Fig. 2e, blue numerals) and two occurred only in NB (Fig. 2e, red numerals). Discrete events were defined by the first date on which Chl exceeded threshold values for the respective basin and were separated by at least 1 day from other exceedance measurements. These events are referred to as "blooms" or "events" throughout the rest of the study. It should be noted that the blooms in NB and SB in April 2011 (events #7–9) were each separated by 2 days and were thus treated as separate events based on the above definition.

Microplankton community composition in both basins was dominated by dinoflagellates (and other flagellated protistan groups), as evidenced by log-transformed dino:diatom ratios > 0 throughout most of the study period (Fig. 3). With the exception of two events (#5 and #7), all blooms were dominated numerically by dinoflagellates in the microplankton (Fig. 3). Euglenids in the genus *Eutreptiella* and dinoflagellates in the genus *Prorocentrum*, *Chaetoceros* spp., and *Akashiwo sanguinea* were numerically dominant species in NB (6.39–21.5%) and SB (7.56–10.33%), comprising of the assemblages, on average, during the study period (Table 3). In SB, additional contributions from *Pseudo-nitzschia* spp. (7.86%) and small gymnodinoid dinoflagellates (7.12%) dominated microplankton composition (Table 3). The contributions of *Eutreptiella* spp. to assemblages in both basins were largely due to a bloom of that species in January 2011 (event

Table 1 General oceanographic conditions in the northern (NB) and southern basins (SB) of King Harbor and Santa Monica Pier (SM Pier, Chl only), California, May 2010–June 2011. Wind speed and upwelling index were measured or derived for the whole area; therefore, a single range is reported. †Minima below the limits of detection

Parameter	Minimum	Maximum	Mean
Temperature (°C)			
NB	12.9	22.6	17.3
SB	12.7	22.1	17.1
Salinity			
NB	28.2	33.4	33.1
SB	29.7	33.5	33.2
Dissolved oxygen (mL L^{-1})			
NB	0.05	9.75	4.30
SB	0.45	8.26	4.20
Chlorophyll fluorescence (μg L^{-1})			
NB	0.34	43.4	2.84
SB	0.56	28.7	2.53
SM Pier	0.20	35.1	6.37
PO_4 (μmol L^{-1})			
NB	0.33	27.7	3.19
SB	0.36	5.13	1.57
$NO_3 + NO_2$ (μmol L^{-1})			
NB	< 0.20†	20.7	7.33
SB	< 0.20†	15.2	6.36
SiO_4 (μmol L^{-1})			
NB	6.90	37.6	17.2
SB	0.36	5.13	8.17
Wind speed (m s^{-1})	0.48	18.4	3.50
Upwelling index (m^3 s^{-1} 100 m^{-1} coastline)	− 3.85	282	91.3

#5; Fig. 3). Overall, SB showed greater assemblage contributions from diatoms in the genera *Chaetoceros*, *Pseudo-nitzschia*, and *Leptocylindrus* than NB (Table 3).

Multivariate analyses show significantly distinct microplankton assemblages in each basin over the study period (SIMPROF, $p < 0.05$; Fig. 4, gray ellipses). These distinct assemblages were driven, in part, by dominance of single taxa, with group I assemblages dominated by *A. sanguinea* and group II assemblages occurring when euglenids were abundant. Assemblages characterized as group III in Fig. 4 primarily occurred when overall biomass was low in each basin. In NB, PO_4 and N:P ratio were the two environmental variables that best explained the differences in assemblage structure over the study period (Bio-Env, $\rho = 0.293$, $p < 0.01$). These variables are presented as bubbles in Fig. 4 and show that group I assemblages (*A. sanguinea*-dominated) in NB were primarily associated with high PO_4 concentrations (black circles) and low N:P (gray circles), while group II (with significant contributions from euglenids) and group III (generally low biomass) generally occurred with low PO_4 concentrations and higher N:P. In SB, temperature and N:P ratio were the two environmental variables that best explained the differences in assemblage structure over the study period (Bio-Env, $\rho = 0.239$, $p < 0.04$). Group I and group III assemblages (*A. sanguinea*- and euglenid-dominated, respectively) tended to occur during periods of higher temperature (white circles), while group II assemblages were more associated with high N:P (gray circles) and relatively lower temperature (Fig. 4). Group I assemblages were, interestingly, also associated with the lowest N:P ratios in the study (Fig. 4).

Table 2 Spearman rank correlation coefficients (ρ) for pairwise comparisons of variables between the northern basin (NB) and southern basin (SB) of King Harbor. Asterisks indicate significant correlations, *$p < 0.05$. **$p < 0.01$

Variable	NB	SB
Temp	0.986**	
Salinity	0.865**	
Diss O_2	0.811**	
Chl	0.538**	
PO_4	0.671**	
NO_3	0.368*	
Si	− 0.114	

Comparisons to Chl and important HAB taxa abundances measured within the harbor to those measured at SM Pier as part of the SCCOOS HAB monitoring program allow us to investigate how King Harbor and larger regional bloom dynamics are coupled. We were not able to detect significant differences ($p > 0.05$) between Chl ($n = 39$; Fig. 5a) at the NB or SB sites in King Harbor and SM Pier with zero time lag for the study period during which data was available for comparison. Additionally, no significant differences in assemblages were evident from multivariate analyses between sites or among seasons (SIMPROF, $p > 0.05$; Fig. 6). When individual HAB taxa that were enumerated across the sites were considered, however, some important relationships became apparent. With zero time lag, abundances of *Prorocentrum* spp. in NB and at SM Pier were weakly correlated between the sites ($\rho = 0.053$, $p < 0.001$; data not shown). When a 1-week lag was applied to the NB and SB datasets, Chl concentrations between SM Pier and SB were positively correlated ($\rho = 0.370$, $p = 0.017$), while the correlation between SM Pier and NB was still weak ($p > 0.05$; Fig. 5b). With a 1-week lag, abundances of *Lingulodinium polyedrum* in both harbor basins and SM Pier were also positively correlated ($\rho = 0.639$–0.696, $p < 0.001$; Fig. 5c), while abundances of *Prorocentrum* spp. ($\rho = 0.386$, $p = 0.005$) and *Pseudo-nitzschia* spp. ($\rho = 0.464$, $p < 0.001$) were correlated only between SM Pier and NB (Fig. 5d, e). Only *Prorocentrum* spp. abundances were correlated between both basins and SM Pier when a 1-week lag to SM Pier was applied (i.e., suggesting movement from King Harbor into Santa Monica Bay, $\rho = 0.400$–0.636, $p < 0.001$, data not shown). Correlations of other HAB taxa abundances between

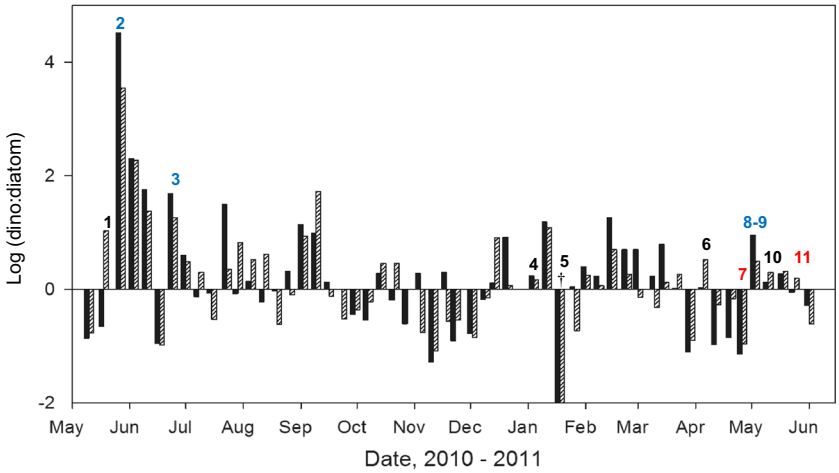

Fig. 3 Log-transformed ratio of dinoflagellate:diatom abundance in NB (black) and SB (gray, hatched) communities from May 2010 to June 2011. †The community on January 18, 2011 was heavily dominated by euglenids of the genus *Eutreptiella*, with no diatom or dinoflagellate species enumerated in the sample. Therefore, the $\log_{10}$(dino:diatom) is undefined and approaches negative infinity. Blue numbers indicate bloom events occurring in only SB, red numbers indicate bloom events occurring in only NB, and black numbers indicate bloom events occurring in both basins

the King Harbor basins and SM Pier were not significant, including *A. sanguinea* ($p = 0.836$), *Alexandrium* spp. ($p = 0.760$), and *Dinophysis* spp. ($p = 0.193$).

Table 3 Average relative abundances (based on numeric abundance) of taxonomic groups contributing ≥ 1% of microplankton community abundance in the northern and southern basins of King Harbor. Dashes indicate groups that contributed < 1% of average microplankton relative abundance in that location during the study period. Standard errors of the mean are presented in parentheses for each taxonomic group

Taxonomic group	Class	Rel. abundance (%)	
		Northern	Southern
Eutreptiella spp.	Euglenophyceae	21.5 (0.03)	9.52 (0.03)
Prorocentrum spp.	Dinophyceae	8.98 (0.02)	9.32 (0.02)
Chaetoceros spp.	Bacillariophyceae	8.97 (0.03)	10.3 (0.02)
Akashiwo sanguinea	Dinophyceae	6.39 (0.03)	7.56 (0.03)
Small gymnodinoids	Dinophyceae	–	7.12 (0.01)
Navicula spp.	Bacillariophyceae	5.42 (0.01)	3.80 (0.01)
Leptocylindrus spp.	Bacillariophyceae	3.78 (0.01)	4.60 (0.02)
Uronema-like ciliate	Oligohymenophorea	3.70 (0.02)	4.20 (0.02)
Putative raphidophyte	Raphidophyceae	3.10 (0.02)	2.16 (0.01)
Scrippsiella spp.	Dinophyceae	2.53 (0.01)	3.51 (0.01)
Pseudo-nitzschia spp.	Bacillariophyceae	2.16 (0.01)	7.86 (0.02)
Silicoflagellates	Actinochrysophyceae	2.00 (0.01)	–
Large gymnodinoids	Dinophyceae	1.89 (0.01)	1.59 (0.01)
Lingulodinium polyedrum	Dinophyceae	1.89 (0.01)	2.61 (0.01)
Dinoflagellate cysts	Dinophyceae	1.68 (0.01)	2.45 (0.01)
Rhizosolenia spp.	Bacillariophyceae	1.66 (0.01)	1.27 (0.01)
Oligotrich ciliates	Spirotrichea	1.27 (0.01)	2.45 (0.01)
Ceratium spp.	Dinophyceae	1.24 (0.01)	2.19 (0.01)

Environmental and Physical Factors Contributing to Blooms

When temperature, nutrient concentrations, tidal amplitude, and wind speed were used as predictor variables of Chl in general linear regression, model solutions for NB included tidal amplitude as a significant predictor only in the 7-day lagged solution (Table 4). Inclusion of tidal amplitude in this model improved overall model fit ($R^2_{Adj} = 0.513$) and reduced root mean square error (RMSE = 0.283) compared to a model that did not include physical processes ($R^2_{Adj} = 0.387$; RMSE = 0.318; Table 4). Temperature was the only other significant predictor of Chl in NB. Phosphate and nitrate were significant predictors of Chl in SB in both the unlagged and 7-day lagged models, and inclusion of tidal amplitude improved model fit ($R^2_{Adj} = 0.449$; RMSE = 0.257) over the instantaneous (i.e., 0 day lagged) model without physical processes included ($R^2_{Adj} = 0.399$; RMSE = 0.269; Table 4). The tidal amplitude regression coefficient was consistently negative in all models (Table 4), suggesting that Chl and tidal amplitude were negatively correlated. Regression models in SB generally had higher fit than those in the NB, with the exception of the 7-day lagged NB model that included tidal amplitude (Table 4). Wind speed was neither a significant predictor in any of the models nor did inclusion of wind speed improve model performance (as increased R^2_{Adj} or decreased RMSE).

The contributions of tidal cycling to variability of Chl and phytoplankton bloom dynamics in both basins were further assessed using continuous wavelet transform and coherence between physical drivers and the continuously measured, corrected, and normalized Chl concentrations. Chl variability showed significant but intermittent 1- and 0.5-day periodicities (Fig. A2), corresponding to dominant harmonics of the semidiurnal tide that characterizes this region. Wavelet coherence

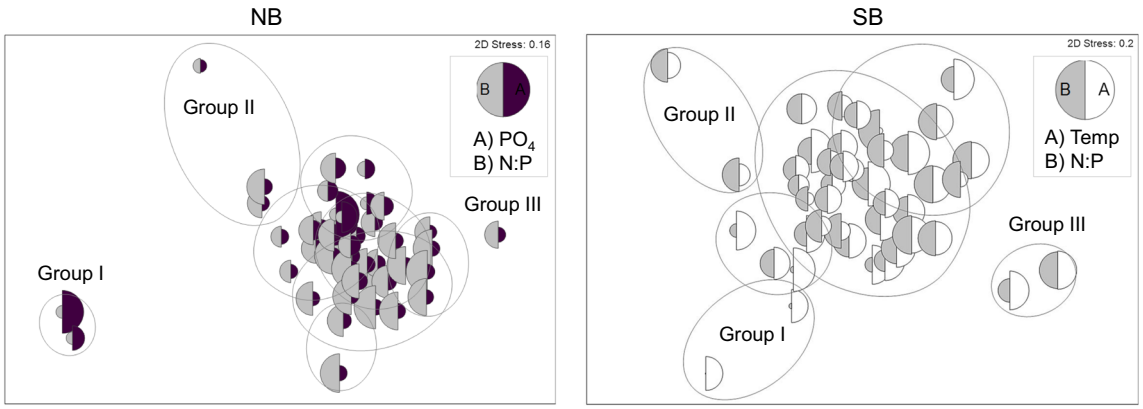

Fig. 4 Non-metric multi-dimensional scaling (nMDS) plots of microplankton assemblages from NB (left) and SB (right). Plankton abundances were square root transformed and resemblances were based on the Bray-Curtis dissimilarity index. Symbols for each sample ($n = 44$ for NB, 43 for SB) are presented as bubbles based on the top two environmental variables that explain the dissimilarities in each set of assemblages (see discussion of BIO-Env in "Results"): dissolved PO_4 (black) and N:P ratio (gray) for NB and temperature (white) and N:P ratio (gray) for SB. Size of the bubble represents linear scales of the normalized variables, i.e., a larger N:P bubble indicates a higher N:P ratio measured for that sample timepoint. Gray ellipses indicate significantly different groups of assemblages with significant differences, based on SIMPROF analysis ($p < 0.05$). Groups (I–III) represent shared characteristics of these assemblages in both NB and SB

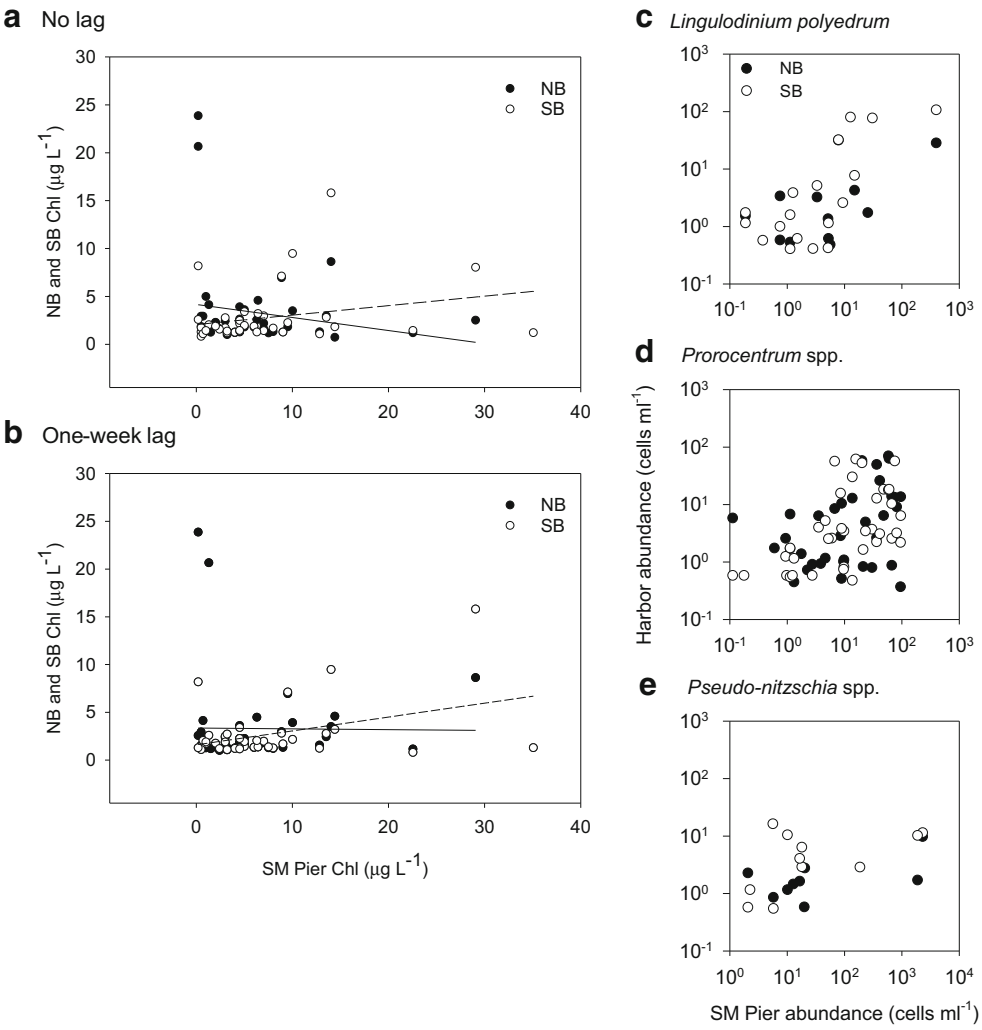

Fig. 5 Scatter plots of Chl with no lag (**a**) and with a 1-week lag (**b**) applied to the King Harbor data in NB (filled circles) and SB (open circles) and at SM Pier (*x*-axis). Scatter plots of abundances for HAB taxa *Lingulodinium polyedrum* (**c**), *Prorocentrum* spp. (**d**), and *Pseudo-nitzschia* spp. (**e**) in King Harbor sites and at SM Pier with a 1-week lag applied to the King Harbor abundances. SM Pier data was obtained from the SCCOOS HAB data portal (http://www.sccoos.org/), and only samples collected within the 3 days prior to the King Harbor samples were used

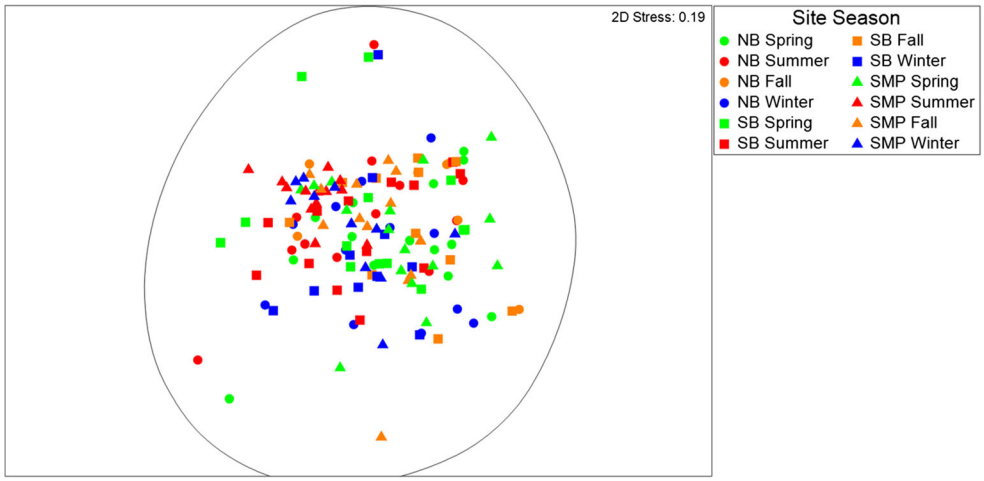

Fig. 6 nMDS plot of HAB taxa assemblages (6 taxa) in King Harbor NB (circles) and SB sites (squares) and at SM Pier (triangles) collected within the 3 days prior to the NB and SB samples (no lag). Data are plotted according to seasons: spring (March–May, black), summer (June–August, dark gray), fall (September–November, light gray), and winter (December–February, open symbol). SM Pier data was obtained from the SCCOOS HAB data portal (http://www.sccoos.org/). Assemblage data were square-root transformed, and the Bray Curtis dissimilarity index was used to build a resemblance matrix. Gray ellipse indicates samples with no significant differences in assemblage, based on SIMPROF analysis ($p < 0.05$)

Table 4 Results from general linear regression analyses of NB and SB weekly Chl with (top) and without (bottom) tidal amplitude as a predictor variable and including zero (0 day) and 1-week (7 days) lagged environmental data. Predictor variable coefficients and p values and model diagnostics (adjusted R^2, root mean square error [RMSE]) are given for each model (with and without tidal amplitude). The three upper Chl data points were trimmed from the dataset (see Table A1 for untrimmed model results). Chl and PO_4 were log-transformed prior to analysis. Upwelling index and salinity were not included in the models given their high level of collinearity with nutrient concentrations and general lack of variability, respectively. All regression models were significant ($p < 0.01$). Asterisks indicate significant predictor variables, *$p < 0.05$ and ** $p < 0.01$, and † indicates $p = 0.050$–0.055

	NB		SB	
	0 day	7 days	0 day	7 days
Predictor variables (w/ tidal amplitude)				
Temperature	0.063*	0.101**	− 0.017	− 0.009
PO_4	0.098	0.032	− 0.350*	− 0.220
Si	0.013	0.019	0.037	0.044
NO_3	− 0.005	0.012	− 0.037*	− 0.071*
Tidal amplitude	*− 0.243*	*− 5.30***	*− 0.182**	*− 1.78*
R^2_{Adj}	0.360	0.513	0.449	0.446
RMSE	0.3250	0.283	0.257	0.258
Predictor variables (no tidal amplitude)				
Temperature	0.074*	0.077*	− 0.018	− 0.017
PO_4	0.153	0.135	− 0.280†	− 0.093
Si	0.016	0.022†	0.042†	0.039
NO_3	− 0.006	0.003	− 0.052*	− 0.088**
R^2_{Adj}	0.303	0.387	0.399	0.442
RMSE	0.3390	0.318	0.269	0.259

spectra showed strong and significant ($p < 0.05$, via area-wise test (Maraun et al. 2007)) correlation of dominant periodicities in Chl and tidal amplitude which were most common in fall–winter (Aug–Dec; Fig. 7a) in NB and in fall–winter and early spring (Jan–Mar 2011) in SB (Fig. 7b). Bloom initiation (gray vertical lines; Fig. 7) occurred during periods when the coherence of tidal amplitude and Chl was minimal (cooler colors) and not statistically significant (areas without bold black outlines; Fig. 7), suggesting blooms began when periodicities of tidal cycle and Chl were less correlated with one another.

Finally, since the upwelling index was not included in the multiple regression models of Chl described above, interactions among upwelling, temperature, nutrient concentrations, and Chl were quantified via bivariate correlation analyses. Spearman rank correlation of untransformed data showed significant positive correlations ($p < 0.05$) of upwelling index with both temperature ($\rho = 0.361$–0.476) and Chl ($\rho = 0.358$–0.604) and significant negative correlations ($p < 0.05$) of upwelling index with nitrate concentrations ($\rho = -0.337$ to -0.296) in both basins.

Discussion

The purpose of the present study was to understand the extent to which local, high-frequency physical processes contribute to phytoplankton blooms in a semi-enclosed harbor in the Southern California Bight, rather than environmental and physical drivers of phytoplankton blooms operating seasonally and/or over multiple years. Several studies in the past decades (Bialonski et al. 2016; Legaard and Thomas 2006; Mantyla et al. 2008; Nezlin and Li 2003; Nezlin et al. 2004; Nezlin

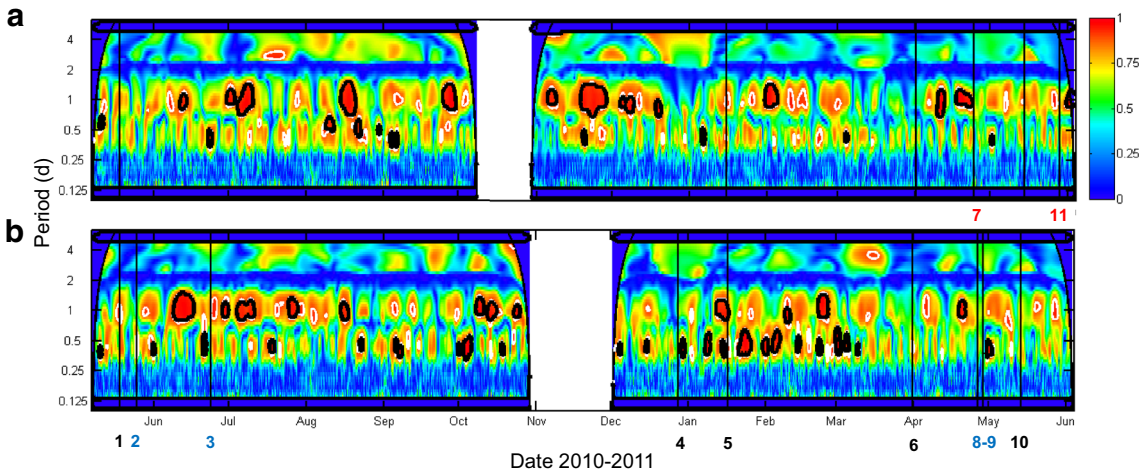

Fig. 7 Wavelet coherence spectra of normalized tidal height and chlorophyll fluorescence from May 2010 to June 2011 in the northern (**a**) and southern (**b**) basins. Warmer colors indicate increased power of the coherence. Thin white contour lines indicate 95% significance using point-wise Monte Carlo simulation against red noise. Thick black contour lines denote significant areas using both point- and area-wise significance tests (see "Methods") and were the areas considered significantly coherent in the present study. Vertical black lines indicate date of initiation of bloom events, and numbers below *x*-axes correspond to bloom event numbers in Figs. 2 and 3. The dark blue-shaded, black line-enclosed curve along the edge of each plot indicates the cone of influence (COI). Data points above the cone were not used in interpretation. Vertical gray lines indicate date of initiation of bloom events, as in Fig. 2

et al. 2012; Shipe et al. 2008) have sought to understand phytoplankton blooms in the Southern California Bight and California Current Ecosystem in the context of upwelling and other large-scale physical and biogeochemical features. Few, however, have studied such dynamics at higher frequencies and in the nearshore environments which may play roles as incubators in larger coastal phytoplankton dynamics (Cloern et al. 2014; Ryan et al. 2008) and in which satellite-based approaches are notoriously difficult (Kahru and Mitchell 1998). Notable exceptions exist. Omand et al. (2012) employed high-frequency (< hourly) data to understand blooms occurring in summer-fall. Other studies used weekly or biweekly data to assess longer term trends in Chl (e.g., Kim et al. 2009) or spatial distributions and connectivity among HAB communities (Bialonski et al. 2016; Shipe et al. 2008). The current study fills a gap in our understanding of phytoplankton blooms in this region by investigating bloom dynamics over the course of a full annual cycle through the use of both high (hourly) and medium (weekly) frequency data in order to resolve changes in overall biomass (Chl) and community structure in the phytoplankton community. Additionally, we have considered locally acting physical processes, including tidal and wind-driven mixing, that are likely affecting phytoplankton biomass and composition in addition to biogeochemical processes in these systems.

Phytoplankton Blooms in King Harbor

Eleven phytoplankton blooms exceeding 2 standard deviations of the mean were identified over the 13-month study period in King Harbor. Given that bloom events #7–9 only lasted 2 days each (Table 3), this bloom frequency (9 blooms [treating events #7–9 as one) in 13 months, or a bloom every 1.44 months) is comparable to the frequency (three blooms in 5 months, or blooms every 1.67 months) observed off Huntington Beach by Omand et al. (2012). This rate of bloom occurrence is also similar to, but more frequent than, the major + minor bloom frequencies observed from the Scripps Pier (5–7 events per year, or blooms every 1.71–2.4 months; Kim et al. 2009) and off the Redondo Beach Pier in Santa Monica Bay (8 blooms over a two-year period, or blooms every 3 months; Seubert et al. 2013). Bloom events in King Harbor occurred primarily in late spring and summer months, with the exception of two events in winter (events #4 and 5; Table 3). These results are also consistent with the 20-year time series at Scripps Pier (Kim et al. 2009), in which the highest frequency of blooms (94% of blooms) observed in spring–summer (shifted to winter–spring after 1994), and with other studies (e.g., Nezlin et al. 2012) that show spring–summer as the period of highest Chl and bloom occurrence in the Southern California Bight.

Only five of the eleven detected bloom events occurred in both harbor basins simultaneously (Fig. 2), and correlation of Chl concentrations between both harbor basins was lower (yet still significant) than correlations of physical environmental variables (Table 2). The two harbor basins both experienced a bloom event (#1) in mid-May 2018 (Fig. 2); yet that event was dominated by diatoms in NB (primarily *Chaetoceros* spp.) and dinoflagellates in SB (primarily *A. sanguinea*; Fig. 3). Microplankton assemblages dominated by *A. sanguinea*, euglenids in the genus *Eutreptiella*, and those with overall low biomass were significantly different from the other assemblages during the study period in each basin (Fig. 4).

Overall, differences in microplankton assemblages in NB and SB were best explained by variability in nutrient concentrations (PO_4 and N:P ratio, primarily) and temperature (in SB). Together, these results suggest a high degree of heterogeneity across the small spatial scale of King Harbor (approx. 0.5 km^2 in total area) which is also reflected in differences in the multivariate drivers of phytoplankton biomass and bloom events (see discussion below).

Physical Processes Contributing to Blooms

Our results revealed significant, yet differential, environmental and physical controls of Chl in King Harbor basins over the course of the study. Nutrient concentrations were not as significant or consistent predictors of biomass or blooms in King Harbor as other studies have reported for coastal waters of the SCB (e.g., Bialonski et al. 2016; Omand et al. 2012; Shipe et al. 2008). Inorganic nutrient concentrations were not significant predictors of biomass in either of the NB models, despite PO_4 concentration and N:P ratio significantly explaining variability in community structure in NB (Fig. 4, and see discussion above). Given the generally higher average concentrations of nutrients in NB than in SB (Table 1), it appears that inorganic nutrients were not the primary factors controlling biomass or bloom development in NB but did contribute to the success of certain species in the assemblages.

In contrast, PO_4 and NO_3 were significant predictors of Chl in SB, although negative regression coefficients for both suggest that dissolved nutrient concentrations measured weekly may not effectively capture the temporal dynamics of nutrient availability and primary producer uptake. Indeed, improved model fit for the 7-day lagged regression results for SB underscore the need for time-lagged nutrient concentrations—not just those collected concomitant with samples for primary producers—to be used in predictions of phytoplankton blooms. These results agree with those of Omand et al. (2012), which showed a strong predictive relationship between NO_3 and phytoplankton blooms observed in San Pedro Bay coastal waters in summer and fall and a 6–10 day lag in the Chl response to nutrient fluxes. N:P ratio, along with temperature, also significantly explained variability in community structure in SB (Fig. 4 and see discussion above). The negative regression of NO_3 and Chl and relationship between N:P and microplankton assemblage may reflect use of other forms of nitrogen (i.e., NH_4, urea, organic N) by the primarily dinoflagellate-dominated blooms in the harbor basins, consistent with documented physiological flexibility in N use (and potential for mixotrophy) by these organisms (as reviewed by Dagenais-Bellefeuille and Morse 2013; Glibert et al. 2016) and the known significant contribution of anthropogenic forms of N to total N in Santa Monica Bay (Howard et al. 2014; Sengupta et al. 2013). The dominance of *A. sanguinea*, a dinoflagellate known to use a variety of reduced forms of N (e.g., Mulholland et al. 2018), in group I assemblages in both basins when N:P ratios were minimal (Fig. 4) supports this interpretation.

Our results also suggest that spatial variability in the strength of these environmental predictors on nearshore phytoplankton blooms is exceptionally high, with connected harbor basins less than 0.25 km apart showing different forms of biogeochemical and physical control. Chl in NB was significantly predicted by temperature (i.e., higher biomass in warmer months) and reduced tidal amplitude in the preceding week (i.e., higher biomass with reduced tidal range). SB Chl was also significantly predicted by tidal amplitude in the non-lagged model (Table 4). Time series analyses underscore these results: wavelet coherence analyses show that bloom initiation occurred during periods when variability in Chl biomass was decoupled from diurnal and semidiurnal periodicities related to the tidal cycle (Fig. 6). Together, these results suggest a release from oscillatory, recurring tidal control when tidal currents and their associated effects on mixing are low, i.e., during periods of neap tide. Indeed, 57% of identified bloom events in NB and 56% of bloom events in SB initiated within 4 days of neap tide in this system. Such effects have been characterized as "tidal stirring," most notably by Cloern (1991) in the San Francisco Bay estuary, and by others in other estuarine ecosystems around the world (Balch 1981; Blauw et al. 2012; Leles et al. 2014; Lucas et al. 1999; Michael et al. 2006; Moser et al. 2017; Sin et al. 1999). However, the effects of tidal stirring on phytoplankton biomass and bloom dynamics in the nearshore reaches of the SCB—where upwelling and oceanographic forcing are considered the norm—have not been highlighted as a driving factor for blooms until now.

Upwelling did not appear to be a significant factor in bloom dynamics within King Harbor. While a significant and positive correlation between upwelling index and Chl was observed in this study, correlations between upwelling index and temperature (positive) or nitrate (negative) were counter those expected from our understanding of the biogeochemical effects of upwelling on coastal water columns (e.g., Palacios et al. 2013). That is, lower temperature and higher nutrient concentrations resulting from upwelling are generally positively correlated with bloom events. This lack of an upwelling signature may be due to a few factors. First, upwelling was generally minimal during the study period, with monthly anomalies indicative of downwelling (i.e., negative) except in a few months during the study period (Fig. 2h, filled circles). Upwelling is not consistent in time or space (Hickey 1979), and the study location lies in a transition zone from lower (south of 33°N) to higher (north of 33°N) influence of upwelling (Macias et al. 2012; Schwing et al. 1996). The seasonal signature of upwelling also appears especially dampened in the nearshore and eastern SCB when compared with other regions in the CCE (Legaard and Thomas 2006; Strub et al. 1990). Second, our results suggest that solar heating in

coastal embayments may be driving covariance among environmental variables, i.e., upwelling, and temperature all increased throughout the spring and summer months, periods when Chl was also high, while nitrate concentrations peaked in late winter (Feb–Mar) when upwelling index and temperature were both low (Fig. 2). Temperature consistently predicted Chl (and was a significant predictor in NB) in multiple regression models in King Harbor and was also an explanatory variable for microplankton community structure in SB. These results are in contrast to observations by Kim et al. (2009) in the southern SCB that temperature does not accurately predict long-term variations in Chl. These results are consistent, however, with observations of temperature as a predictor of blooms in an offshore location in Santa Monica Bay, approximately 30 km from our study site (Shipe et al. 2008), again highlighting the spatial heterogeneity of processes affecting phytoplankton in the SCB.

Finally, our observations of a relatively minor role for upwelling in the biogeochemistry in King Harbor is also consistent with the substantial contributions of anthropogenic sources to total N in the Santa Monica Bay region of the SCB (Howard et al. 2014; Sengupta et al. 2013). Anthropogenic N sources would predominantly be in the form of NH_4 delivered from publicly owned water treatment works (POTWs) rather than river runoff, which is limited to the fall–spring wet season (Howard et al. 2014; Sengupta et al. 2013). This delivery of N to the SCB has been shown to stimulate growth of phytoplankton—primarily dinoflagellates—and especially as it mixes with coastal water masses (Reifel et al. 2013). However, NH_4 concentrations were not measured in the current study, so we can only conclude that the nitrate (and likely other forms of N) that was a significant predictor of the primarily dinoflagellate blooms in the southern basin of King Harbor was likely delivered by processes other than upwelling or was being recycled within the harbor itself (i.e., by nitrification). Taken as a whole, our results suggest that, in the semi-enclosed waters of King Harbor, upwelling plays a less significant and less direct role in stimulating growth of phytoplankton than in waters further offshore or in different regions of Santa Monica Bay and the SCB.

Regional Implications

The current study was not able to quantify the physical or biogeochemical drivers of phytoplankton biomass or blooms outside of King Harbor during the study period, so it is not possible to determine what, if any, components of the observed dynamics are directly attributable to advective transport between King Harbor and Santa Monica Bay. However, by comparing Chl and important HAB taxa abundances measured within the harbor and at SM Pier as part of the SCCOOS HAB monitoring program, some similarities between bloom dynamics in the harbor and the larger region were observed. Chl in SB, NB, and at SM Pier was similar in overall magnitude, although the generally higher minima in King Harbor likely reflect less nutrient-limited growth than offshore. Chl in SB and at SM Pier was significantly correlated when a 1-week lag was applied to the harbor data, suggesting a potential transport of primary producer biomass from Santa Monica Bay into the more open basin (SB) of King Harbor. SB also showed greater importance of inorganic nutrients in predicting Chl (see discussion, above), suggesting that, of the two basins, SB may operate more like the adjacent coastal ocean.

Abundances of shared HAB taxa also shed some light on the potential relationship between King Harbor bloom dynamics and those in Santa Monica Bay. Multivariate analyses of HAB taxa did not show any significant differences in assemblages between King Harbor and SM Pier over the whole dataset (Fig. 6), and the abundances of several HAB taxa (*Alexandrium* spp., *A. sanguinea*, and *Dinophysis* spp.) were not significantly correlated between the two regions. In contrast, *Pseudo-nitzschia* spp. and *Prorocentrum* spp. were significantly correlated between SM Pier and NB when a 1-week lag was applied to the harbor data, suggesting a potentially offshore origin for these taxa (Fig. 5). Onshore transport of *Pseudo-nitzschia* spp. from offshore areas of origin is suggested to occur via internal waves associated with periods of upwelling relaxation (Shanks et al. 2014) and have been observed in other studies in the SCB (Seegers et al. 2015). Bialonski et al. (2016) also showed a southward transport of *Prorocentrum* spp., from SM Pier to Newport Pier in San Pedro Bay. However, it is also worth noting that dinoflagellates in the genus *Prorocentrum* were present in over 60% of the King Harbor and 100% of the SM Pier samples. It is therefore possible that correlations in abundances of this HAB taxa (with or without time lags) reflect its persistent presence throughout Santa Monica Bay.

Abundances of *Lingulodinium polyedrum* were also positively correlated between both basins in King Harbor and SM Pier when a 1-week lag was applied to the harbor data. This correlation may indicate onshore transport or that the processes controlling the success of *L. polyedrum* in the nearshore (harbor) and coastal (pier) locations are similar. Unlike *Pseudo-nitzschia*, blooms of *L. polyedrum* are often quite visible in nearshore waters (Moorthi et al. 2006). Studies have also suggested a role for upwelling relaxation (and the potential onshore transport that entails, McCabe et al. 2015) in stimulation of *L. polyedrum* blooms (Smayda 2010) and wind-driven drift of warm surface waters in the maintenance of these blooms (Ruiz-de la Torre et al. 2013). It is therefore possible that these species may be further transported towards nearshore waters via similar mechanisms as for *Pseudo-nitzschia*; however, greater spatial resolution would be required to determine if this is, in fact, driving the lagged, positive correlation of *L. polyedrum* in these two areas.

These results suggest the potential for King Harbor—and other nearshore embayments—to serve as a reservoir for HAB species and phytoplankton, more broadly, transported in from Santa Monica Bay and the SCB. The dinoflagellate species which show evidence for onshore transport in this study (*Prorocentrum* spp. and *L. polyedrum*) are also both known to produce temporary (ecdysal) or resting cysts (Figueroa and Bravo 2005; Grzebyk and Berland 1996). It is therefore possible that, once cyst banks in these nearshore waters are established, they may persist and seed future HABs in the region. To better understand bloom dynamics—both within nearshore environments such as King Harbor and in the larger coastal ocean—requires a more highly resolved understanding of the physical and biogeochemical processes controlling phytoplankton biomass and community composition in space and time in these systems.

Acknowledgments The authors thank J.M. Rose for assistance in statistical analyses, R.A. Schaffner for assistance in mapping, and B.H. Jones for helpful conversations on the analyses of time series data. The authors also gratefully acknowledge L. Darjany, A.G. Gellene, C. Oberg, E.L. Seubert, A. Schnetzer, and P.E. Connell for technical assistance conducting the field work and assistance in collection and processing of samples. This study was made possible with the help of the City of Redondo Beach Fire Department, the Los Angeles County Lifeguards, the King Harbor Marina operators, and the City of Redondo Beach, who provided invaluable site access and logistical support. This paper is dedicated to the memory of Scott Duke-Sylvester, a colleague who left us too soon and who provided guidance in revising the statistical analyses in this study.

Funding Information This research was supported by the National Science Foundation (Award #CCR-0120778 to D.A.C. and G.S.S.). Manuscript writing was supported by the National Academies for Science, Engineering, and Medicine Gulf Research Program Early Career Fellowship (Award #2000009659 to B.A.S).

References

Abi-Khalil, C., C. Lopez-Joven, E. Abadie, V. Savar, Z. Amzil, M. Laabir, and J.-L. Rolland. 2016. Exposure to the paralytic shellfish toxin producer Alexandrium catenella increases the susceptibility of the oyster *Crassostrea gigas* to pathogenic Vibrios. *Toxins* 8: 24.

Akmajian, A.M., J.J. Scordino, and A. Acevedo-Gutiérrez. 2017. Year-round algal toxin exposure in free-ranging sea lions. *Marine Ecology Progress Series* 583: 243–258.

Anderson, D., P. Hoagland, Y. Kaoru, and A. W. White. 2000. Estimated annual economic impacts from harmful algal blooms (HABs) in the United States. Woods Hole Oceanographic Institution Technical Report: WHOI-2000–2011. Woods Hole, MA: Woods Hole Oceanogr Inst.

Anderson, D.M., P.M. Glibert, and J.M. Burkholder. 2002. Harmful algal blooms and eutrophication: Nutrient sources, composition, and consequences. *Estuaries* 25: 704–726.

Babin, M., J. Cullen, C. Roesler, P.L. Donaghay, G.J. Doucette, M. Kahru, M. Lewis, C.A. Scholin, M. Sieracki, and H. Sosik. 2005. New approaches and technologies for observing harmful algal blooms. *Oceanography* 18: 210–227.

Balch, W.M. 1981. An apparent lunar tidal cycle of phytoplankton blooming and community succession in the Gulf of Maine. *Journal of Experimental Marine Biology and Ecology* 55: 65–77.

Bialonski, S., D.A. Caron, J. Schloen, U. Feudel, H. Kantz, and S.D. Moorthi. 2016. Phytoplankton dynamics in the Southern California Bight indicate a complex mixture of transport and biology. *Journal of Plankton Research* 38: 1077–1091.

Blauw, A.N., E. Benincà, R.W.P.M. Laane, N. Greenwood, and J. Huisman. 2012. Dancing with the tides: fluctuations of coastal phytoplankton orchestrated by different oscillatory modes of the tidal cycle. *PLoS One* 7: e49319.

Bray, J.R., and J.T. Curtis. 1957. An ordination of the upland forest communities of southern Wisconsin. *Ecological Monographs* 27: 325–349.

Brody, S.R., M.S. Lozier, and J.P. Dunne. 2013. A comparison of methods to determine phytoplankton bloom initiation. *Journal of Geophysical Research: Oceans* 118: 2345–2357.

Carey, C.C., P.C. Hanson, R.C. Lathrop, and A.L.St. Amand. 2016. Using wavelet analyses to examine variability in phytoplankton seasonal succession and annual periodicity. *Journal of Plankton Research* 38: 27–40.

Carstensen, J., P. Henriksen, and A.-S. Heiskanen. 2007. Summer algal blooms in shallow estuaries: definition, mechanisms, and link to eutrophication. *Limnology and Oceanography* 52: 370–384.

Clarke, K.R., and R.N. Gorley. 2015. PRIMER v7: User manual/tutorial. Plymouth PRIMER-E U.K.

Clarke, K.R., R.N. Gorley, P.J. Somerfield, and R.M. Warwick. 2014. *Change in marine communities: an approach to statistical analysis and interpretation*. 3nd ed. Plymouth: PRIMER-E.

Cloern, J.E. 1991. Tidal stirring and phytoplankton bloom dynamics in an estuary. *Journal of Marine Research* 49: 203–221.

Cloern, J.E., S.Q. Foster, and A.E. Kleckner. 2014. Phytoplankton primary production in the world's estuarine-coastal ecosystems. *Biogeosciences* 11: 2477–2501.

Clough, J., and S. Strom. 2005. Effects of *Heterosigma akashiwo* (Raphidophyceae) on protist grazers: laboratory experiments with ciliates and heterotrophic dinoflagellates. *Aquatic Microbial Ecology* 39: 121–134.

Cole, H.S., A.P. Martin, A. Yool, and S. Henson. 2015. Basin-wide mechanisms for spring bloom initiation: How typical is the North Atlantic? *ICES Journal of Marine Science* 72: 2029–2040.

Colin, S.P., and H.G. Dam. 2003. Effects of the toxic dinoflagellate *Alexandrium fundyense* on the copepod *Acartia hudsonica*: a test of the mechanisms that reduce ingestion rates. *Marine Ecology-Progress Series* 248: 55–65.

Corcoran, A.A., and R.F. Shipe. 2011. Inshore-offshore and vertical patterns of phytoplankton biomass and community composition in Santa Monica Bay, CA (USA). *Estuarine, Coastal and Shelf Science* 94: 24–35.

Cullen, J. 2008. Observation and prediction of harmful algal blooms, in Real-Time Coastal Observing Systems for Marine Ecosystem Dynamics and Harmful Algal Blooms: Theory, Instrumentation and Modelling, eds M. Babin, et al. (Paris: UNESCO), 1–41.

Dagenais-Bellefeuille, S., and D. Morse. 2013. Putting the N in dinoflagellates. *Frontiers in Microbiology* 4: 369–369.

Doney, S.C., M. Ruckelshaus, J.E. Duffy, J.P. Barry, F. Chan, C.A. English, H.M. Galindo, J.M. Grebmeier, A.B. Hollowed, N. Knowlton, J. Polovina, N.N. Rabalais, W.J. Sydeman, and L.D. Talley. 2012. Climate change impacts on marine ecosystems. *Annual Review of Marine Science* 4: Null.

Doucette, G.J., and R.M. Kudela. 2017. Chapter twelve in situ and real-time identification of toxins and toxin-producing microorganisms in the environment. In *Recent Advances in the Analysis of Marine Toxins*, 411–443.

Egerton, T.A., R.E. Morse, H.G. Marshall, and M.R. Mulholland. 2014. Emergence of algal blooms: The effects of short-term variability in

water quality on phytoplankton abundance, diversity, and community composition in a tidal estuary. *Microorganisms* 2 (1): 33–57.

Fernandes, L.F., K.A. Hubbard, M.L. Richlen, J. Smith, S.S. Bates, J. Ehrman, C. Leger, L.L. Mafra Jr., D. Kulis, M. Quilliam, K. Libera, L. McCauley, and D.M. Anderson. 2014. Diversity and toxicity of the diatom *Pseudo-nitzschia peragallo* in the Gulf of Maine, northwestern Atlantic Ocean. *Deep Sea Res Part 2 Top Stud Oceanogr* 103: 139–162.

Figueroa, R.I., and I. Bravo. 2005. Sexual reproduction and two different encystement strategies of *Lingulodinium polyedrum* (Dinophyceae) in culture. *Journal of Phycology* 41: 370–379.

Fritsch, F.N., and R.E. Carlson. 1980. Monotone piecewise cubic interpolation. *SIAM Journal on Numerical Analysis* 17: 238–246.

Ganju, N.K., M.J. Brush, B. Rashleigh, A.L. Aretxabaleta, P. Del Barrio, J.S. Grear, L.A. Harris, S.J. Lake, G. McCardell, J. O'Donnell, D.K. Ralston, R.P. Signell, J.M. Testa, and J.M. Vaudrey. 2016. Progress and challenges in coupled hydrodynamic-ecological estuarine modeling. *Estuaries and Coasts: Journal of the Estuarine Research Federation* 39 (2): 311–332.

Glibert, P.M., J.I. Allen, A.F. Bouwman, C.W. Brown, K.J. Flynn, A.J. Lewitus, and C.J. Madden. 2010. Modeling of HABs and eutrophication: status, advances, challenges. *Journal of Marine Systems* 83: 262–275.

Glibert, P.M., F.P. Wilkerson, R.C. Dugdale, J.A. Raven, C.L. Dupont, P.R. Leavitt, A.E. Parker, J.M. Burkholder, and T.M. Kana. 2016. Pluses and minuses of ammonium and nitrate uptake and assimilation by phytoplankton and implications for productivity and community composition, with emphasis on nitrogen-enriched conditions. *Limnology and Oceanography* 61: 165–197.

Graham, S., and S. Strom. 2010. Growth and grazing of microzooplankton in response to the harmful alga *Heterosigma akashiwo* in prey mixtures. *Aquatic Microbial Ecology* 59: 111–124.

Grinsted, A., J.C. Moore, and S. Jevrejeva. 2004. Application of the cross wavelet transform and wavelet coherence to geophysical time series, *Nonlin. Processes Geophys* 11: 561–566. https://doi.org/10.5194/npg-11-561-2004.

Grzebyk, D., and B. Berland. 1996. Influences of temperature, salinity and irradiance on growth of *Prorocentrum minimum* (Dinophyceae) from the Mediterranean Sea. *Journal of Plankton Research* 18: 1837–1849.

Hallegraeff, G.M. 2010. Ocean climate change, phytoplankton community responses, and harmful algal blooms: a formidable predictive challenge. *Journal of Phycology* 46: 220–235.

Heisler, J., P.M. Glibert, J.M. Burkholder, D.M. Anderson, W. Cochlan, W.C. Dennison, Q. Dortch, C.J. Gobler, C.A. Heil, E. Humphries, A. Lewitus, R. Magnien, H.G. Marshall, K. Sellner, D.A. Stockwell, D.K. Stoecker, and M. Suddleson. 2008. Eutrophication and harmful algal blooms: a scientific consensus. *Harmful Algae* 8 (1): 3–13.

Hickey, B.M. 1979. The California current system—hypotheses and facts. *Progress in Oceanography* 8: 191–279.

Ho, J.C., and A.M. Michalak. 2015. Challenges in tracking harmful algal blooms: a synthesis of evidence from Lake Erie. *Journal of Great Lakes Research* 41: 317–325.

Howard, M.D.A., M. Sutula, D.A. Caron, Y. Chao, J.D. Farrara, H. Frenzel, B. Jones, G. Robertson, K. McLaughlin, and A. Sengupta. 2014. Anthropogenic nutrient sources rival natural sources on small scales in the coastal waters of the Southern California bight. *Limnology and Oceanography* 59: 285–297.

Hu, C., F.E. Muller-Karger, C. Taylor, K.L. Carder, C. Kelble, E. Johns, and C.A. Heil. 2005. Red tide detection and tracing using MODIS fluorescence data: a regional example in SW Florida coastal waters. *Remote Sensing of Environment* 97: 311–321.

Imai, I. 2012. Biology and ecology of harmful algal blooms (20): interactions between red tide plankton species - 1. *Aquabiology (Tokyo)* 34: 160–167.

Kahru, M., and B.G. Mitchell. 1998. Spectral reflectance and absorption of a massive red tide off Southern California. *Journal of Geophysical Research-Oceans* 103: 21601–21609.

Kaitala, S. 2019. Development of the operational observation system of harmful algal blooms as a BOOS project. Copenhagen: ICES.

Kim, H.-J., A.J. Miller, J. McGowan, and M.L. Carter. 2009. Coastal phytoplankton blooms in the Southern California bight. *Progress in Oceanography* 82: 137–147.

Kudela, R.M., S. Seeyave, and W.P. Cochlan. 2010. The role of nutrients in regulation and promotion of harmful algal blooms in upwelling systems. *Progress in Oceanography* 85: 122–135.

Lefebvre, K.A., L. Quakenbush, E. Frame, K.B. Huntington, G. Sheffield, R. Stimmelmayr, A. Bryan, P. Kendrick, H. Ziel, T. Goldstein, J.A. Snyder, T. Gelatt, F. Gulland, B. Dickerson, and V. Gill. 2016. Prevalence of algal toxins in Alaskan marine mammals foraging in a changing arctic and subarctic environment. *Harmful Algae* 55: 13–24.

Legaard, K.R., and A.C. Thomas. 2006. Spatial patterns in seasonal and interannual variability of chlorophyll and sea surface temperature in the California current. *Journal of Geophysical Research: Oceans* 111. C06032, https://doi.org/10.1029/2005JC003282.

Leles, S., C. Alves-de-Souza, C. de Oliveira Faria, A. Beatriz Ramos, A. Macedo Fernandes, and G. Aparecida de Oliveira Moser. 2014. Short-term phytoplankton dynamics in response to tidal stirring in a tropical estuary (southeastern Brazil). *Brazilian Journal of Oceanography* 62: 341–349.

Lewitus, A.J., R.A. Horner, D.A. Caron, E. Garcia-Mendoza, B.M. Hickey, M. Hunter, D.D. Huppert, R.M. Kudela, G.W. Langlois, J.L. Largier, E.J. Lessard, R. RaLonde, J.E. Jack Rensel, P.G. Strutton, V.L. Trainer, and J.F. Tweddle. 2012. Harmful algal blooms along the north American west coast region: History, trends, causes, and impacts. *Harmful Algae* 19: 133–159.

Lucas, L.V., J.R. Koseff, J.E. Cloern, S.G. Monismith, and J.K. Thompson. 1999. Processes governing phytoplankton blooms in estuaries. I: the local production-loss balance. *Marine Ecology Progress Series* 187: 1–15.

Macias, D., M.R. Landry, A. Gershunov, A.J. Miller, and P.J.S. Franks. 2012. Climatic control of upwelling variability along the Western north-American coast. *PLoS One* 7: e30436.

Mantyla, A.W., S.J. Bograd, and E.L. Venrick. 2008. Patterns and controls of chlorophyll-a and primary productivity cycles in the Southern California bight. *Journal of Marine Systems* 73: 48–60.

Maraun, D., J. Kurths. 2004. Cross wavelet analysis: significance testing and pitfalls. *Nonlinear Processes in Geophysics, European Geosciences Union (EGU)*, 11 (4), pp.505–514. ffhal-00302384f

Maraun, D., J. Kurths, and M. Holschneider. 2007. Nonstationary Gaussian processes in wavelet domain: Synthesis, estimation and significance testing. *Physical Review E* 75: 016707.

McCabe, R.M., B.M. Hickey, E.P. Dever, and P. MacCready. 2015. Seasonal cross-shelf flow structure, upwelling relaxation, and the alongshelf pressure gradient in the northern California current system. *Journal of Physical Oceanography* 45: 209–227.

Michael, S.W., C.H. Kenneth, J.L. Alan, L.W. Jennifer, and L.W. David. 2006. Variability in phytoplankton pigment biomass and taxonomic composition over tidal cycles in a salt marsh estuary. *Marine Ecology Progress Series* 320: 109–120.

Miller, M.A., R.M. Kudela, A. Mekebri, D. Crane, S.C. Oates, M.T. Tinker, M. Staedler, W.A. Miller, S. Toy-Choutka, C. Dominik, D. Hardin, G. Langlois, M. Murray, K. Ward, and D.A. Jessup. 2010. Evidence for a novel marine harmful algal bloom: Cyanotoxin (microcystin) transfer from land to sea otters. *PLoS One* 5: e12576.

Moorthi, S.D., P.D. Countway, B.A. Stauffer, and D.A. Caron. 2006. Use of quantitative real-time PCR to investigate the dynamics of the red tide dinoflagellate *Lingulodinium polyedrum*. *Microbial Ecology* 52 (1): 136–150.

Moser, G.A.O., F.R. Piedras, A.B.J. Oaquim, D.S. Souza, S.G. Leles, D.T. de Lima, A.B.A. Ramos, C.d.O. Farias, and A.M. Fernandes. 2017. Tidal effects on phytoplankton assemblages in a near-pristine estuary: a trait-based approach for the case of a shallow tropical ecosystem in Brazil. *Marine Ecology* 38: e12450.

Mulholland, M.R., R. Morse, T. Egerton, P.W. Bernhardt, and K.C. Filippino. 2018. Blooms of dinoflagellate mixotrophs in a lower Chesapeake Bay tributary: carbon and nitrogen uptake over diurnal, seasonal, and interannual timescales. *Estuaries & Coasts* 41: 1744–1765.

Nezlin, N.P., and B.L. Li. 2003. Time-series analysis of remote-sensed chlorophyll and environmental factors in the Santa Monica-San Pedro Basin off Southern California. *Journal of Marine Systems* 39: 185–202.

Nezlin, N.P., J.J. Oram, P.M. DiGiacomo, and N. Gruber. 2004. Subseasonal to interannual variations of sea surface temperature, salinity, oxygen anomaly, and transmissivity in Santa Monica Bay, California from 1987 to 1997. *Continental Shelf Research* 24: 1053–1082.

Nezlin, N.P., M.A. Sutula, R.P. Stumpf, and A. Sengupta. 2012. Phytoplankton blooms detected by SeaWiFS along the central and southern California coast. *Journal of Geophysical Research: Oceans*: 117. C07004, https://doi.org/10.1029/2011JC007773.

O'Neil, J.M., T.W. Davis, M.A. Burford, and C.J. Gobler. 2012. The rise of harmful cyanobacteria blooms: the potential roles of eutrophication and climate change. *Harmful Algae* 14: 313–334.

Omand, M.M., F. Feddersen, R.T. Guza, and P.J.S. Franks. 2012. Episodic vertical nutrient fluxes and nearshore phytoplankton blooms in Southern California. *Limnology and Oceanography* 57: 1673–1688.

Omand, M.M., J.J. Leichter, P.J.S. Franks, R.T. Guza, A.J. Lucas, and F. Feddersen. 2011. Physical and biological processes underlying the sudden surface appearance of a red tide in the nearshore. *Limnology and Oceanography* 56: 787–801.

Orrico, C.M., C. Moore, D. Romanko, A. Derr, A.H. Barnard, C. Janzen, N. Larson, D. Murphy, R. Johnson, and J. Bauman. 2007. WQM: a new integrated water quality monitoring package for long-term in-situ observation of physical and biogeochemical parameters. In Oceans 2007 MTS/IEEE Vancouver.

Paerl, H.W., W.S. Gardner, K.E. Havens, A.R. Joyner, M.J. McCarthy, S.E. Newell, B. Qin, and J.T. Scott. 2016. Mitigating cyanobacterial harmful algal blooms in aquatic ecosystems impacted by climate change and anthropogenic nutrients. *Harmful Algae* 54: 213–222.

Palacios, D.M., E.L. Hazen, I.D. Schroeder, and S.J. Bograd. 2013. Modeling the temperature-nitrate relationship in the coastal upwelling domain of the California Current. *Journal of Geophysical Research: Oceans* 118: 3223–3239.

Place, A.R., H.A. Bowers, T.R. Bachvaroff, J.E. Adolf, J.R. Deeds, and J. Sheng. 2012. *Karlodinium veneficum*—the little dinoflagellate with a big bite. *Harmful Algae* 14: 179–195.

Rabalais, N.N., R.E. Turner, R.J. Diaz, and D. Justić. 2009. Global change and eutrophication of coastal waters. *ICES Journal of Marine Science* 66: 1528–1537.

Ralston, D.K., M.L. Brosnahan, S.E. Fox, K. Lee, and D.M. Anderson. 2015. Temperature and residence time controls on an estuarine harmful algal bloom: modeling hydrodynamics and *Alexandrium fundyense* in Nauset estuary. *Estuaries and coasts : journal of the Estuarine Research Federation* 38 (6): 2240–2258.

Reifel, K.M., A.A. Corcoran, C. Cash, R. Shipe, and B.H. Jones. 2013. Effects of a surfacing effluent plume on a coastal phytoplankton community. *Continental Shelf Research* 60: 38–50.

Ruiz-de la Torre, M.C., H. Maske, J. Ochoa, and C.O. Almeda-Jauregui. 2013. Maintenance of coastal surface blooms by surface temperature stratification and wind drift. *PLoS One* 8: e58958.

Ryan, J.P., A.M. Fischer, R.M. Kudela, J.F.R. Gower, S.A. King, R. Marin, and F.P. Chavez. 2009. Influences of upwelling and downwelling winds on red tide bloom dynamics in Monterey Bay, California. *Continental Shelf Research* 29: 785–795.

Ryan, J.P., J.F.R. Gower, S.A. King, W.P. Bissett, A.M. Fischer, R.M. Kudela, Z. Kolber, F. Mazzillo, E.V. Rienecker, and F.P. Chavez. 2008. A coastal ocean extreme bloom incubator. *Geophysical Research Letters* 35. L12602, https://doi.org/10.1029/2008GL034081.

Ryan, J.P., R.M. Kudela, J.M. Birch, M. Blum, H.A. Bowers, F.P. Chavez, G.J. Doucette, K. Hayashi, R. Marin III, C.M. Mikulski, J.T. Pennington, C.A. Scholin, G.J. Smith, A. Woods, and Y. Zhang. 2017. Causality of an extreme harmful algal bloom in Monterey Bay, California, during the 2014–2016 Northeast Pacific warm anomaly. *Geophysical Research Letters* 44: 5571–5579.

Schnetzer, A., P.E. Miller, R.A. Schaffner, B.A. Stauffer, B.H. Jones, S.B. Weisberg, P.M. DiGiacomo, W.M. Berelson, and D.A. Caron. 2007. Blooms of *Pseudo-nitzschia* and domoic acid in the San Pedro Channel and Los Angeles harbor areas of the Southern California Bight, 2003-2004. *Harmful Algae* 6: 372–387.

Schwing, F.B., M. O'Farrell, J.M. Steger, and K. Baltz. 1996. Coastal upwelling indices west coast of North America 1946–1995, ed. N.O.a.A.A. U.S. Dept. of Commerce, National Marine Fisheries Service, 32.

Seegers, B.N., J.M. Birch, R. Marin, C.A. Scholin, D.A. Caron, E.L. Seubert, M.D.A. Howard, G.L. Robertson, and B.H. Jones. 2015. Subsurface seeding of surface harmful algal blooms observed through the integration of autonomous gliders, moored environmental sample processors, and satellite remote sensing in southern California. *Limnology and Oceanography* 60: 754–764.

Sengupta, A., M. Sutula, K. McLaughlin, M. Howard, L. Tiefenthaler, and T. Von Bitner. 2013. Terrestrial nutrient loads and fluxes to the Southern California Bight, USA. Southern California Coastal Water Research Project 2013 Annual Report, 245e258.

Seubert, E.L., A.G. Gellene, M.D. Howard, P. Connell, M. Ragan, B.H. Jones, J. Runyan, and D.A. Caron. 2013. Seasonal and annual dynamics of harmful algae and algal toxins revealed through weekly monitoring at two coastal ocean sites off southern California, USA. *Environmental Science and Pollution Research International* 20 (10): 6878–6895.

Shanks, A.L., S.G. Morgan, J. Macmahan, A. Reniers, M. Jarvis, J. Brown, A. Fujimura, and C. Griesemer. 2014. Onshore transport of plankton by internal tides and upwelling-relaxation events. *Marine Ecol. Prog. Ser.* 502: 39–51.

Shipe, R.F., A. Leinweber, and N. Gruber. 2008. Abiotic controls of potentially harmful algal blooms in Santa Monica Bay, California. *Continental Shelf Research* 28: 2584–2593.

Siegel, D.A., S.C. Doney, and J.A. Yoder. 2002. The North Atlantic spring phytoplankton bloom and Sverdrup's critical depth hypothesis. *Science* 296 (5568): 730–733.

Sin, Y., R.L. Wetzel, and I.C. Anderson. 1999. Spatial and temporal characteristics of nutrient and phytoplankton dynamics in the York River Estuary, Virginia: analyses of long-term data. *Estuaries* 22: 260–275.

Smayda, T.J. 1997. What is a bloom? A commentary. *Limnology and Oceanography* 42: 1132–1136.

Smayda, T.J. 2010. Adaptations and selection of harmful and other dinoflagellate species in upwelling systems 1. Morphology and adaptive polymorphism. *Progress in Oceanography* 85: 53–70.

Smith, J., P. Connell, R.H. Evans, A.G. Gellene, M.D.A. Howard, B.H. Jones, S. Kaveggia, L. Palmer, A. Schnetzer, B.N. Seegers, E.L. Seubert, A.O. Tatters, and D.A. Caron. 2018. A decade and a half of *Pseudo-nitzschia* spp. and domoic acid along the coast of southern California. *Harmful Algae* 79: 87–104.

Soares, M.C.S., M.M. Marinho, S.M.O.F. Azevedo, C.W.C. Branco, and V.L.M. Huszar. 2012. Eutrophication and retention time affecting

spatial heterogeneity in a tropical reservoir. *Limnologica* 42: 197–203.

Stauffer, B.A., A.G. Gellene, A. Schnetzer, E.L. Seubert, C. Oberg, G.S. Sukhatme, and D.A. Caron. 2012. An oceanographic, meteorological and biological 'perfect storm' yields a massive fish kill. *Marine Ecology - Progress Series* 468: 231–243.

Stauffer, B.A., A. Schnetzer, A.G. Gellene, C. Oberg, G.S. Sukhatme, and D.A. Caron. 2013. Effects of an acute hypoxic event on microplankton community structure in a coastal harbor of Southern California. *Estuaries and Coasts* 36: 135–148.

Stauffer, B.A., H.A. Bowers, E. Buckley, T.W. Davis, T.H. Johengen, R. Kudela, M.A. McManus, H. Purcell, G.J. Smith, A. Vander Woude, and M.N. Tamburri. 2019. Considerations in harmful algal bloom research and monitoring: perspectives from a consensus-building workshop and technology testing. *Frontiers in Marine Science* 6: 399. https://doi.org/10.3389/fmars.2019.00399.

Stauffer BA, Gellene AG, Schnetzer A, Seubert EL, Oberg C, Sukhatme GS, Caron DA (2012) An oceanographic, meteorological, and biological 'perfect storm' yields a massive fish kill. *Mar Ecol Prog Ser* 468: 231–243. https://doi.org/10.3354/meps09927.

Stauffer, B.A., A.G. Gellene, D. Rico, C. Sur, and D.A. Caron. 2017. Grazing of the heterotrophic dinoflagellate *Noctiluca scintillans* on dinoflagellate and raphidophyte prey. *Aquatic Microbial Ecology* 80: 193–207.

Strickland, J. D. H. and T. R. Parsons. 1972. A practical handbook of seawater analysis, 2nd ed. Fisheries Research Board of Canada Bulletin No. 167, Ottawa.

Strub, P.T., C. James, A.C. Thomas, and M.R. Abbott. 1990. Seasonal and nonseasonal variability of satellite-derived surface pigment concentration in the California Current. *Journal of Geophysical Research: Oceans* 95: 11501–11530.

Todd, R.E., D.L. Rudnick, and R.E. Davis. 2009. Monitoring the greater San Pedro Bay region using autonomous underwater gliders during fall of 2006. *Journal of Geophysical Research* 114: C06001.

Torrence, C. and G.P. Compo, 1998: A practical guide to wavelet analysis. *Bull. Amer. Meteor. Soc* 79: 61–78. https://doi.org/10.1175/1520-0477(1998)079<0061:APGTWA>2.0.CO;2

Trainer, V.L., G.C. Pitcher, B. Reguera, and T.J. Smayda. 2010. The distribution and impacts of harmful algal bloom species in eastern boundary upwelling systems. *Progress in Oceanography* 85: 33–52.

Turner, J.T., and P.A. Tester. 1997. Toxic marine phytoplankton, zooplankton grazers, and pelagic food webs. *Limnology and Oceanography* 42: 1203–1214.

Utermohl, H. 1931. Neue Wege in der quantitativen Erfassung des Plankton. *Verhandlungen der Internationalen Vereinigung fuer Theoretische Limnologie Stuttgart* 5: 567–596.

Utermohl, H. 1958. Zur Gewassertypenfrage tropischer Seen. *Verhandlungen Internationalen Vereinigung Limnologie* 13 (1): 236–251.

Weissbach, A., M. Rudstrom, M. Olofsson, C. Bechemin, J. Icely, A. Newton, U. Tillmann, and C. Legrand. 2011. Phytoplankton allelochemical interactions change microbial food web dynamics. *Limnology and Oceanography* 56: 899–909.

Wilcox, R.R. 2003. *Applying contemporary statistical techniques*. New York: Academic Press.

Xu, N., Y.Z. Tang, J. Qin, S. Duan, and C.J. Gobler. 2015. Ability of the marine diatoms *Pseudo-nitzschia multiseries* and *P. pungens* to inhibit the growth of co-occurring phytoplankton via allelopathy. *Aquatic Microbial Ecology* 74: 29–41.

Zeng, L., and D. Li. 2015. Development of in situ sensors for chlorophyll concentration measurement. *Journal of Sensors* 2015: 16.